ACTIVE HEAT EXCHANGE SYSTEM DEVELOPMENT FOR LATENT HEAT THERMAL ENERGY STORAGE

TOPICAL REPORT

Joseph Alario, Robert Kosson, and Robert Haslett
Grumman Aerospace Corporation
Bethpage, New York 11714

January 1980

Prepared for

for

ACTIVE HEAT EXCHANGE
SYSTEM DEVELOPMENT FOR
LATENT HEAT THERMAL ENERGY STORAGE

Joseph Alario, Robert Kosson, and Robert Haslett
Grumman Aerospace Corporation
Bethpage, New York 11714

January 1980

TABLE OF CONTENTS

LIST OF ILLUSTRATIONS

LIST OF ILLUSTRATIONS (Contd)

1.0 INTRODUCTION

Thermal energy storage is a promising method for extending the steam generating capabilities of both conventional fossil fuel power plants and advanced solar thermal energy conversion systems. Excess thermal energy available from the steam boiler (or concentrating solar collector) can be stored during off-peak demand periods and then used to increase steam capacity during peak load periods. In a solar application, this stored energy would be substituted for the primary energy source during nonsunlight periods.

Thermal energy can be stored as the heat required to induce a temperature change, a phase transformation (e.g., solid to liquid), or a chemical change in a suitable medium. Using the latent heat of fusion (phase change) is attractive because the heat absorbed per pound of storage material is relatively high, resulting in a more compact system. Molten salts and salt eutectics are particularly attractive as phase change media because of their high weight and volumetric heat storage capabilities, their abundance in nature and as the result of industrial processes, and their low cost per unit storage capability.

A preceding study for NASA-Lewis (Reference 1) showed that a latent thermal energy storage system which utilized a conventional passive tube and shell heat exchanger for salt containment was both technically and economically feasible. The study revealed that suitable latent heat media were inexpensive and that a major portion of the cost was related to the passive heat exchange process. The accumulation of salt deposits on discharge tube surfaces, combined with a high thermal resistance of the solid Phase Change Material (PCM), required a large (and costly) heat exchanger surface area.

Significant performance and cost benefits can be realized if active heat exchange concepts can be developed which prevent the buildup of a solid salt layer on the heat

transfer surfaces. This program was initiated to design and test two active heat exchange concepts for latent heat thermal energy storage systems suitable to the utility industry. Test modules will be designed for a storage capacity of 10 kWh_t and a heat transfer rate of 10 kW_t. These systems, if cost effective, can play an important part in enhancing our nations dwindling energy resources.

2.0 SUMMARY

The overall objective of this program is the development of an active heat exchange process in a latent heat thermal energy storage (TES) system which is suitable for utility applications. These include either conventionally fueled plants or advanced solar central receiver power plants. An effective TES system would be used to supply peak energy requirements with energy stored during the off-peak periods. For conventional power plants this offsets the need to increase the plant boiler capacity, whereas advanced solar power plants require thermal energy storage for buffering during normal operation and as the primary energy source during nonsunlight hours.

The program organization consists of multiple tasks culminating in hardware demonstration and recommendation for future larger scale development efforts. Specific tasks involve concept selection, including the TES media; detailed design and analysis of laboratory-scale test units; hardware fabrication; test evaluation, and data analysis and recommendations. This topical report presents the results of the concept selection phase of the program and briefly describes the design of two recommended demonstration test modules.

General performance requirements for the test modules are a storage capacity of 10 kWh_t and a heat transfer rate of 10 kW_t. With a suitable choice of storage media the systems would be capable of generating steam over the temperature range 250°C to 400°C, although in this case the boiling temperature was specified between 315°C and 350°C for compatibility with advanced solar central receiver power plants.

At these temperatures suitable phase change materials are confined to molten salts and salt eutectics. The evaluation of the candidate materials considered the following criteria: melting point, latent heat of fusion, heat storage capacity (kWh_t/unit volume), corrosion characteristics, handling problems, availability and cost. Of the candidate salts considered, three families were found best suited for

this TES application: chlorides, hydroxides and nitrates. The specific salts recommended, in order of preference, were as follows:

1. 20.5KCL • 24.5NaCl • 55.0MgCl$_2$, % by weight – A chloride salt eutectic that melts at 385°C (725°F).

2. KOH – Potassium hydroxide, melting point at 360°C (680°F)

3. NaNO$_3$ – Sodium nitrate, melting point at 307°C (585°F)

All three salts have good thermal performance, few corrosion problems – which permits the use of less expensive containment materials (e.g., mild steel), and they are available in large quantities at a reasonable cost. The chloride salt eutectic was selected for the demonstration test evaluation since it best fits the steam generating requirement (350°C) of advanced solar power plants.

Two active heat exchange concepts were selected for demonstration hardware development:

* Direct contact heat exchanger
* Rotating drum with fixed scraper

These were selected from among the various concepts considered (scrapers, agitators, vibrators, slurries) because they exhibited the best combination of low development risk and high cost benefit. Unit cost estimates for the chosen TES concepts as applied to a 300 MW$_t$ utility application with 6 hr of storage are presented below.

	Unit Cost ($/kWh$_t$)
Passive tube-shell	21
Direct contact HX	16
Rotating drum	16

The development test modules are designed to interface with an intermediate heat transport loop which uses a liquid metal eutectic (44.5Pb/55.5Bi% by wt.) as the fluid. Three separate tank modules are provided: 1) a liquid metal tank which serves as a supply reservoir and contains the pump, 2) a molten salt tank which contains the PCM supply and a pump, and 3) a central heat exchange module within which the heat transfer between the molten salt and liquid metal occurs. Both heat exchange concepts

are primarily made with 1020 mild steel and both use a nitrogen gas blanket to prevent atmospheric contamination of the salt.

The direct contact heat exchange concept is illustrated in Figure 2-1. Three tank modules are coupled by two separate fluid loops; one for the molten salt, the other for the liquid metal carrier. The salt serves as the thermal energy storage medium, while the liquid metal transfers the stored energy to the eventual heat sink, in this case an open water loop. Separate streams of salt and liquid metal, which emanate from their respective tanks, are mixed together in the heat exchange reservoir. Both latent and sensible heat are transferred to the cooler liquid metal by the countercurrent flow of molten salt bubbles which are injected at the bottom of the metal column. As the salt solidifies, it rises to the top of the heat exchange reservoir, where it is directed over the edges, falling to the bottom of the surrounding tank. It is held here until the next charging cycle, when it is melted (by electrical heaters which simulate the heat source) and drained into the molten salt tank. Another discharge cycle can then begin.
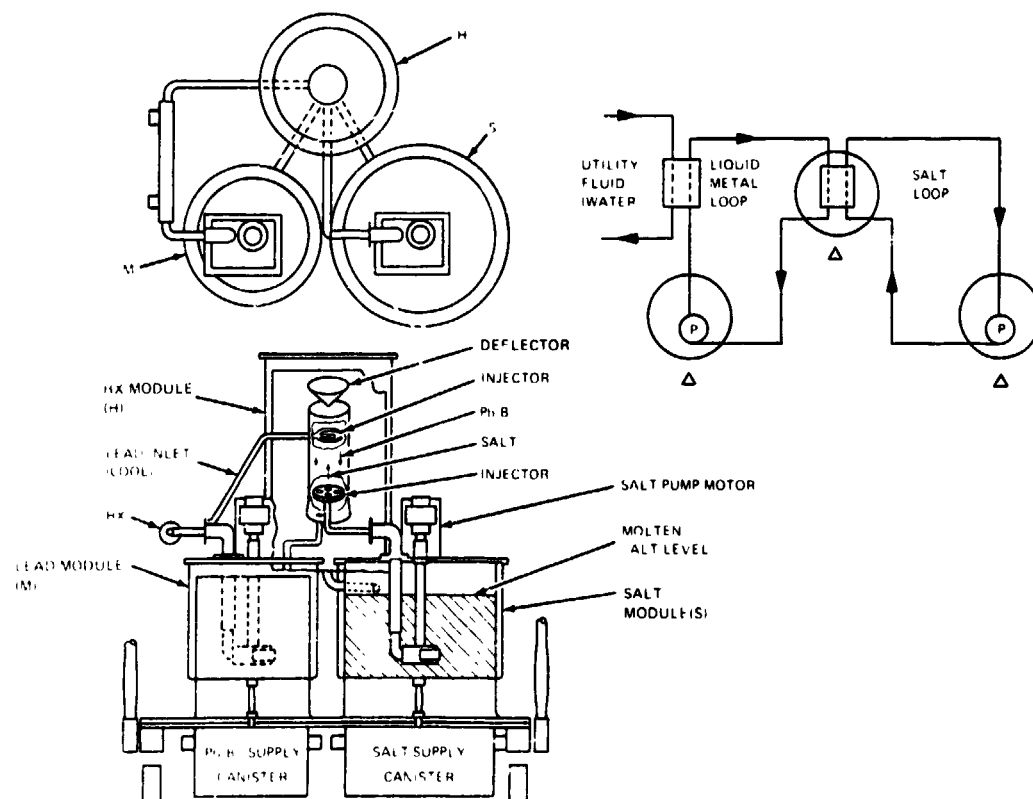
Figure 2-1 Direct Contact HX Concept

2-3

The rotating drum concept in Figure 2-2 is designed to take advantage of all of the hardware (tanks, plumbing, pumps, instrumentation, etc.) used for the direct contact heat exchange concept. Only one-half of the central heat exchange module need be replaced to convert from one system to the other. In this concept, the heat exchange between the molten salt and the liquid metal takes place on the circumference of a rotating hollow steel drum. Molten salt sprays onto the outside surface, while the cooler liquid metal flows through a narrow internal annulus. As heat is removed, the salt solidifies and adheres to the outside surface. Located 270 degrees from the salt admission point in the direction of rotation, a fixed scraper blade removes the solid salt layer. The electroless nickel plating on the drum minimizes the surface adhesion strength and permits easier scraping.

1767-0CR(T)
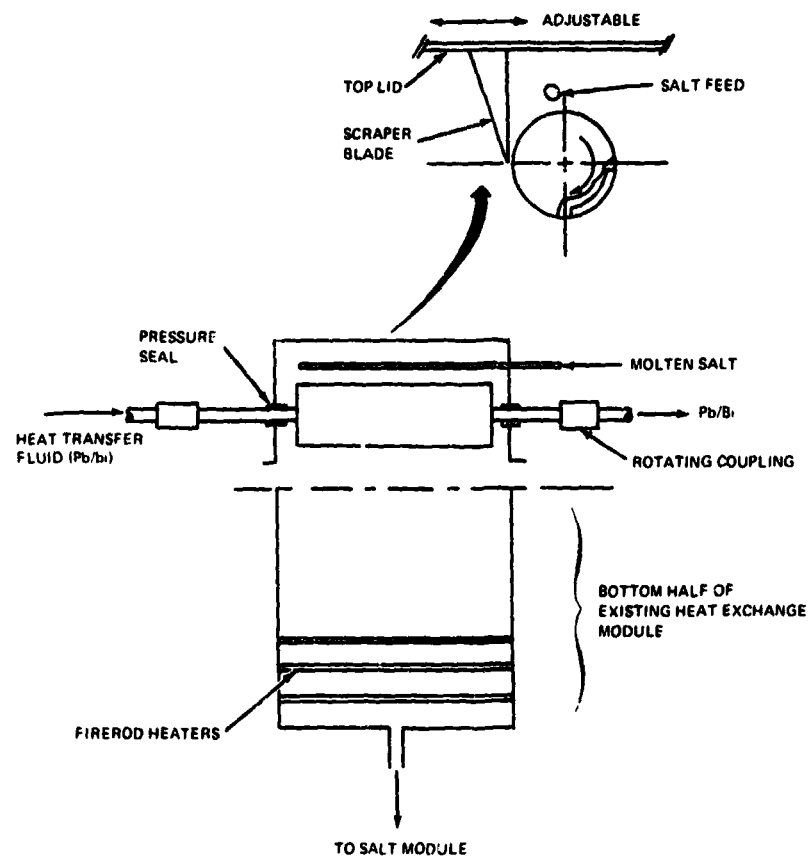
Figure 2-2 Rotating Drum Heat Exchanger Concept

The following sections of this report present the supporting details for the salt selection, identification and evaluation of all the heat exchanger concepts, and a description of the recommended systems.

2-4

3.0 THERMAL ENERGY STORAGE (TES) MEDIA SELECTION

Storage media or salts chosen for the TES system will have a significant impact on the overall design. Candidate salts must be stable, possess good thermal physical properties, be compatible with relatively low-cost contaminant materials, and not separate into constituent components over the system life (20-30 yr). Desirable thermal-physical properties include a high latent heat of fusion 0.06 - 0.13 kWh/kg (100-200 Btu/lb) reasonable thermal conductivity 1.7 - 3.5 W/m°C (1-2 Btu/hr ft°F) and specific heat (0.2-0.5 Cal/g°C), a low vapor pressure ($<$ 1 mmHg), and a moderate density change between the liquid and solid phases (10-20%). The overall system cost will dictate whether or not the design is accepted by the utility industry. The system must compete with a number of alternatives including increased boiler size, electrical energy storage, and sensible heat storage. Hence, it is critical that salts be carefully screened in order to select the lowest cost salts that are also compatible with low-cost containment materials, such as stainless steels, in order to develop a marketable product.

3.1 CANDIDATE SALTS

A basic consideration in choosing a suitable medium for latent heat thermal energy storage applications is the desired working temperature. In this study the TES heat exchange system is used to produce boiling in a steam power cycle, which requires that the melting temperature match the boiling requirements of the cycle. For example, consider a typical supercritical fossil plant which is representative of modern installations. Figure 3-1 shows the steam requirements and how a latent TES system would be used to provide boiling for an auxiliary power supply. Steam to provide energy for storage is available at 540°C, 24 MPa (1000°F, 3600 psi) and would be cooled and condensed to pressurized water at 374°C during the TES charging cycle. During discharge to the auxiliary powercycle, the TES system would supply the energy needed for boiling at 260°C.

For the purposes of this study and to provide a general data base, the candidate storage media included a wide range of melting points between 250°C (480°F) and (650°C) 1200°F. Salts in the following generic families can be considered for applications within this temperature range: fluorides, chlorides, hydroxides, nitrates/nitrites,

carbonates, sulfates, and oxides. As summarized in Figure 3-2, chlorides, hydroxides, and nitrates/nitrites were selected for further consideration.
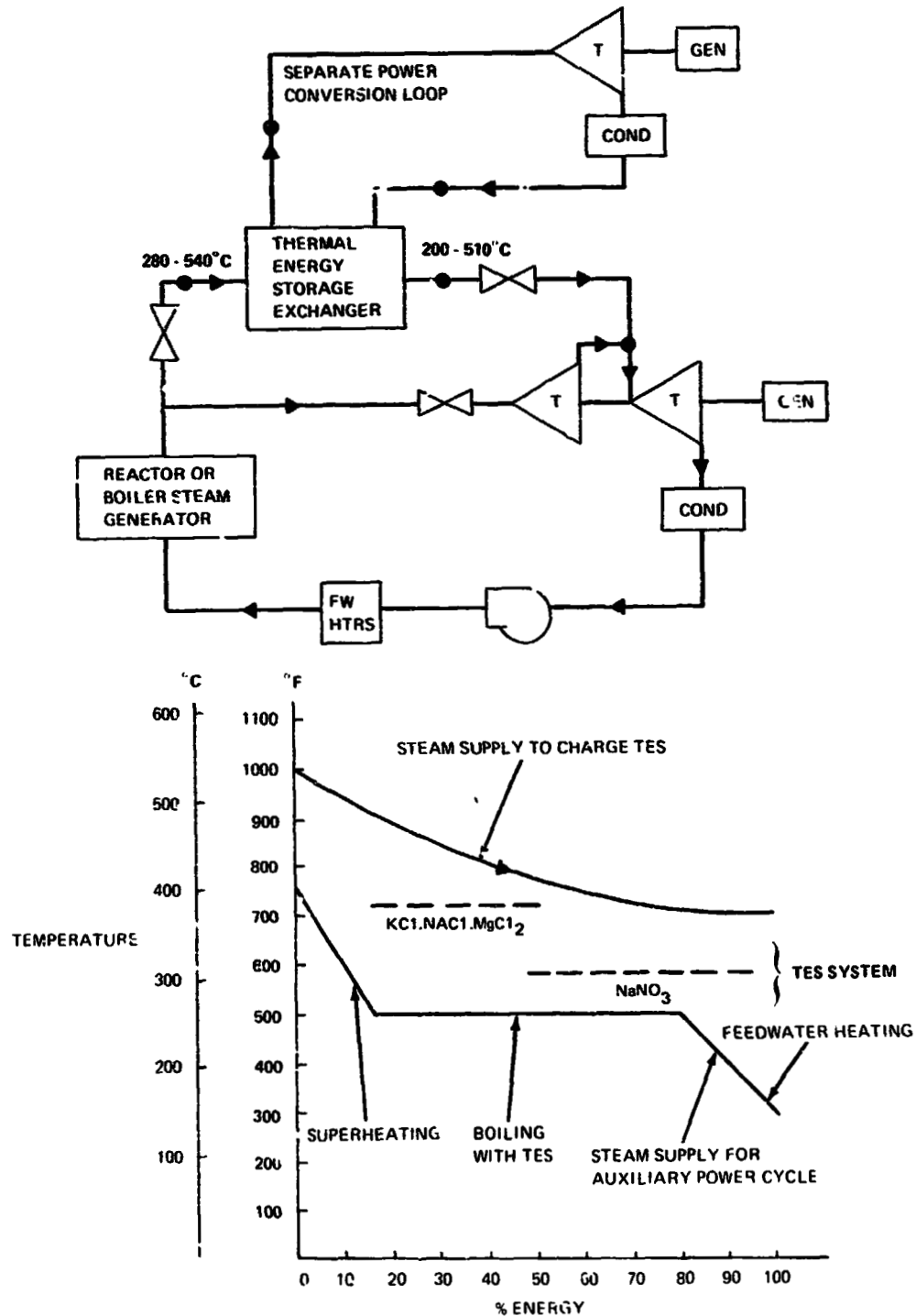
1767-003(T)

Figure 3-2 Latent TES Storage for Fossil Fuel
Auxiliary Power Cycle

	RECOMMENDED	REJECTED	COMMENTS
FLUORIDES		X	ONLY FLUORIDE SALTS WHICH MELT BELOW 500°C CONTAIN LARGE AMOUNTS OF EXPENSIVE Li, Be, OR ALKALI METAL; FLUORIDES NOT AVAILABLE IN LARGE QUANTITIES REQUIRED
CHLORIDES	X		LOW COST, GOOD THERMAL PROPERTIES; AVAILABLE IN SUFFICIENT QUANTITIES FOR UTILITY APPLICATIONS
HYDROXIDES	X		LOW COST, GOOD THERMAL PROPERTIES; AVAILABLE IN SUFFICIENT QUANTITIES FOR UTILITY APPLICATIONS
NITRATES/NITRITES	X		LOW COST, GOOD THERMAL PROPERTIES; AVAILABLE IN SUFFICIENT QUANTITIES FOR UTILITY APPLICATIONS
CARBONATES		X	APPLICABLE TEMPERATURE RANGE > 850°F FOR WHICH CHEAPER CHLORIDE SALTS EXIST
SULFATES		X	HIGHLY CORROSIVE
OXIDES		X	HIGHLY CORROSIVE

1767-004(T)

Figure 3-2 Salt Selection Summary

3.1.1 Fluorides

In general, fluorides possess the best thermal properties of the salts under consideration, and they have received a great deal of attention in prior studies (References 2,3, and 4). For the present study fluorides were rejected mainly on the basis of cost and availability. According to Reference 3, the only fluoride eutectics which melt below 500°C (1000°F) must contain large amounts of LiF, BeF_2 or MBF_4 (where M = alkali metal). BeF_2 is expensive and highly toxic. MBF_4 has a significant vapor pressure and can be extremely corrosive even to high nickel content alloys. LiF is expensive and in short supply.

Even modest power plant size systems could require 10 million lb of salt per installation. Foote Mineral, the largest manufacturer of LiF (and of Li salts of all kinds), reported that their potential annual production capacity is only 4 million lb per year. For this reason, the near term use of LiF for TES is not practical. Use of fluoride salts must wait for TES systems which store large amounts of heat above 649°C (1200°F), a temperature which exceeds the requirements of contemplated central solar systems.

3.1.2 Carbonates

Reference 5 recommends carbonates over chlorides and hydroxides as heat storage salts. However, all of the recommended eutectics which melt below 538°C (1000°F) contain large percentages of Li_2CO_3. The same cost and availability problems which apply to LiF also apply to Li_2CO_3, although to a slightly lesser degree. This is unfortunate because carbonates have good thermal properties. Moreover, the presence of Li_2CO_3 has been shown to form a passivating layer on steels which results in very low corrosion rates. Reference 3 lists a eutectic mix of 57% K_2CO_3 and 43% $MgCO_3$ which melts at 460°C (860°F) and might be suitable; however, it would be more expensive than a chloride eutectic which melts at 465°C (869°F) and has a higher heat of fusion.

3.1.3 Sulfates

A sulfate (Glauber's salt) $Na_2SO_4 \bullet 10H_2O$ is being used by G. E. in its low temperature rotating drum system (Reference 6). For this study, sulfates were rejected because of their extremely corrosive nature at higher temperatures. When heated, sulfates give off O_2 and form sulfides which result in rapid steel corrosion (Reference 3). An oxygen atmosphere has been suggested to retard sulfide formation, but the presence of pressurized O_2 would result in many practical problems in a real system.

3.1.4 Oxides

Oxides were also rejected because they are corrosive and generally difficult to purify.

3.1.5 Chlorides

While they do not have thermal properties quite as attractive as fluorides, chlorides have good properties and are cheap and available in large quantities. Several of the recommended eutectics are chlorides. The principal chlorides of general interest to TES are Na, K, Mg, Ba, and Ca. $ZnCl_2$ has been eliminated because of its relatively high cost and since it has a tendency to subcool.

Containment of chlorides depends critically on the purity of the melt. Water, even if present in only minute amounts, will cause excessive corrosion. References 7

and 8, however, indicate that some chlorides can be contained in mild steel if they are dry and pure. In particular, Reference 8 tested a eutectic of $NaCL \bullet KCl \bullet MgCl_2$ in 1020 mild steel for 1000 hr at 500°C and noted no intergranular or mass transfer corrosion. Blanket atmospheres of N_2, Ar or He have been used successfully to prevent atmospheric contamination.

Some undesirable features of chlorides are that $MgCl_2$ and $CaCl_2$, when strongly heated, give off toxic fumes which would be a problem if a TES unit ruptures. Also, chlorides have a very large volume change on fusion; for example, for NaCl the volume change from solid to liquid is 25%, so that significant salt movement will occur during cycling. $CaCl_2$ is a desiccant, so that an exothermic reaction will occur if it contacts water. $Mg(OH)_2$ contamination of $MgCl_2$ results in the formation of oxichloride cement (MgOCl) which could be a problem.

3.1.6 Hydroxides

Hydroxides are also available in large quantities at a relatively low cost and are therefore potential TES salts. A non-eutectic mix of NaOH (91%), $NaNO_3$ (8%), and 1% unspecified corrosion control additives is marketed under the name "Thermkeep" [R] by Comstock and Wescott, Inc. at a cost of about $0.20 per lb.

Two contaminants that pose a corrosion problem in NaOH are H_2O and CO_2, which can be absorbed from the atmosphere. Use of a blanket atmosphere is essential and References 3 and 5 recommend H_2, although Reference 3 notes that this introduces possible long-term problems with hydrogen embrittlement of the alloys and weldments of the containment unit. Noting the danger of explosion inherent in a pressurized H_2 atmosphere, Reference 9 suggests that satisfactory results might be obtained using a mixture of 10% H_2 and 90% N_2 which would reduce the risk. Reference 5 questions the seriousness of CO_2 contamination and points out some contradictions in existing data regarding water contamination. Most authorities (References 10 and 5) suggest using stainless steel. However, Comstock and Westcott use mild steel in their "Thermkeep" [R] system made possible by their use of a corrosion inhibitor. Also, corrosion problems may be expected to be worse for KOH than NaOH (Reference 5).

Hydroxides are extremely hydroscopic and any contact with water would result in a highly exothermic reaction (possibly explosive in nature) which would be quite

troublesome. In addition, hydroxides are caustic and could be a danger to personnel in the vicinity of a ruptured container. According to Reference 8, NaOH may give off toxic fumes when strongly heated.

Thermal properties of hydroxides are not as good as those of chlorides. It should be noted that NaOH, in addition to a solid-liquid transformation at 321°C (610°F) which has a ΔH_{fs} = 38 cal/gm, also exhibits a solid-solid phase transformation at 296°C (565°F) with an additional ΔH=38 cal/gm.

3.1.7 Nitrates

While the thermal properties of nitrate/nitrite eutectics are not as good as those of chlorides and hydroxides, the low costs, good corrosion properties, and low melting points make them good candidates for TES applications. The specific salts considered are: KNO_3, $NaNO_3$ and $NaNO_2$.

Eutectic mixtures of these three salts have been available under various trade names as heat transfer fluids since the late 1930s (U-TEC-TIC, HITEC, HTS, Partherm). Reference 11 describes a 143°C (290°F) melting point eutectic called "HTS," which is identical to HITEC, Partherm 290, and U-TEC-TIC (References 12 and 13). Fairly complete data is available for these salts because of their long use.

Nitrates/nitrites are superior to most salts in that they form a passivating layer on steels by the formation of surface oxide layers. Moreover, the presence of small amounts of water does not appear to increase the corrosion rate significantly (Reference 3). Kirst, et al, gives a corrosion rate on mild steel of 0.0003 in./month at 454°C (850°F) (Reference 11). Most corrosion problems will result from solid impurities in the melt, particularly Na_2SO_4 and Al oxides. A blanketing atmosphere of N_2 is recommended by several sources (References 9 and 11).

Nitrites do not pose some of the hazards associated with other salts; they evolve no toxic gases nor are they caustic. They should, however, be kept out of contact with organic matter (fire hazard), cyanide, and aluminum. At temperatures above 454°C (849°F), nitrites continuously degrade by $5 NaNO_2 \rightarrow 3NaNO_3 + Na_2O + N_2$. This represents the upper limit to which these salts are useful and care should be taken to prevent nitrite-containing TES units from overheating. Baker Chemical lists the

decomposition point of $NaNO_3$ as 380°C (716°F). Compared to chlorides, nitrates present much less of a problem from volume change on fusion, the increase for $NaNO_3$ being 10.7%, that for KNO_3 only 3.3% and that for $NaNO_2$ less than 20% (Reference 10).

3.2 PROPERTY AND COST DATA

Figure 3-3 presents a list of thermophysical property data for candidate media based on the use of chloride, hydroxide, and nitrate/nitrite salts in the primary temperature range of interest, 250-500°C, for conventional power plants. Similar data for higher melting point salts which could be used in higher temperature central solar power plants are presented in Figure 3-4. Vapor pressure for each of the listed salts is less than 1 mmHg.

Salt costs as well as thermophysical and chemical properties will impact the salt selection for a full-scale system implementation. There are two cost considerations associated with the choice of a particular salt. The first and most obvious is the bulk cost of the required material in a purified condition. The second consideration is the impact of the selection on the required system hardware such as the size and construction of storage tanks, heat exchangers, pumps and plumbing. Only the cost of the bulk material will be considered here.

Various chemical suppliers were contacted to obtain salt prices for the quantities required for a typical power plant application. Because some degree of purification beyond commercial grade will be required, this additional expense must be considered in estimating the total TES cost and at least a preliminary estimate must be included in any realistic system cost appraisal. The purification cost was estimated as follows: First, suppliers of salt in large quantities were contacted including Foote Mineral, Croton Chemical Company, Morton Salt, Hooker Chemical and Plastics Corporation, Dow Chemical, and IMC Chemical Group. In general, it was found that the purity of commercial grade salts ranges from 90 - 99.5% (not including water of crystallization) with a variety of impurities. For example, in the case of $MgCl_2 \bullet 6H_2O$ and $CaCl_2 \bullet 2H_2O$, 50% and 20% H_2O, respectively, is contained in the crystal lattice. Consultants were retained in order to determine which of the various impurities might pose a problem and require removal. It was concluded that water and oxygen are critical contaminants and that water must be removed from salts to the maximum degree

SALT ELEMENT A·B·C	MELT POINT °C (°F)	COMPOSITION WEIGHT %			HEAT OF FUSION, ΔH_{fs} CAL/GM (BTU/LB)	SPECIFIC HEAT CAL/GM°C		THERMAL CONDUCTIVITY 10^3 X CAL/SEC °C CM (BTU/HR FT °F)		DENSITY GM/CC (LB/FT³)		HEAT STORAGE KW-HR/FT³
		A	B	C		SOLID (C_{ps})	LIQUID (C_{pl})	SOLID (k_s)	LIQUID (k_l)	SOLID (ρs)	LIQUID (ρ_l)	
$NaNO_3 \cdot NaOH$	246 (475)	84.5	15.5	—	42.6 (76.5)	.45	.45	1.56 (.377)	1.56 (.377)	2.24 (140)	1.933 (120.7)	3.14
$NaCl \cdot NaNO_3$	297 (567)	4.6	95.4	—	46.8 (84)	.44	.43	1.46 (.35)	1.46 (.35)	2.26 (141)	1.88 (117)	3.47
$NaNO_3$	307 (585)	100	—	—	43.5 (78.1)	.45	.44	1.35 (.33)	1.45 (.35)	2.26 (141)	1.90 (119)	3.23
NaOH	318 (605)	100	—	—	76 (136)	.48	.50	2.20 (.53)	2.20 (.53)	2.83 (180)	1.76 (108)	7.05
$KCl \cdot KNO_3$	320 (608)	4.5	95.5	—	26.21 (47)	.28	.29	1.15 (.278)	1.15 (.278)	2.11 (132)	1.85 (116)	1.82
KOH	360 (680)	100	—	—	32.1 (57.6)	.32	.36	2.20 (.53)	2.20 (.53)	2.04 (127)	1.73 (108)	2.14
$KCl \cdot NaCl \cdot MgCl_2$	385 (725)	14.5	22.3	63.2	70.3 (126)	.23	.248	3.6–3.8 (.87–.92)	1.9–2.4 (.47–.59)	2.25 (140)	1.63 (102)	5.17
$NaCl \cdot BaCl_2 \cdot MgCl_2$	418 (784)	28.4	31.8	39.8	81.6 (146)	.19	.21	3.6–3.8 (.87–.92)	1.9–2.4 (.47–.59)	2.76 (172)	2.12 (132)	7.38
$NaCl \cdot MgCl_2$	450 (842)	60	40	—	111 (199)	.22	.24	3.6–3.8 (.87–.92)	2.27 (.55)	2.23 (139.1)	1.61 (100)	8.11
$CaCl_2 \cdot KCl \cdot NaCl$	465 (869)	64.5	6.5	29	77.6 (139)	.21	.23	3.6–3.8 (.87–.92)	1.9–2.4 (.47–.59)	2.15 (134)	1.85 (115)	5.46
$NaCl \cdot CaCl_2$	500 (928)	33	67	—	67 (121)	.20	.24	3.6–3.8 (.87–.92)	2.44 (.59)	2.16 (134)	1.89 (118)	4.75
$KCl \cdot NaCl \cdot CaCl_2$	504 (939)	5	29	66	67 (120)	.26	.24	3.6–3.8 (.87–.92)	2.39 (.58)	2.15 (134)	1.90 (119)	4.71

1767-005(T)

Figure 3-3 Candidate Salts for Conventional Power Plant Applications

SALT	MELT POINT °C (°F)	COMPOSITION WEIGHT, %			HEAT OF FUSION, ΔH$_{FS}$ (BTU/LB) CAL/GM	SPECIFIC HEAT CAL/GM°C, BTU/LB°F		THERMAL CONDUCTIVITY 10³ X CAL/SEC°C CM (BTU/HR FT°F)		DENSITY GM/CC (LB/FT³)		HEAT STORAGE KW-HR/FT³
		A	B	C		SOLID (C$_{ps}$)	LIQUID (C$_{pm}$)	SOLID (k$_s$)	LIQUID (k$_l$)	SOLID (ρ$_s$)	LIQUID (ρ$_l$)	
KCl · Na₂CO₃	587 (1088)	49 3	50 7	–	75 8 (136)	235	306	6 3 (1 5)	6 3 (1 5)	2.46 (153)	1 74 (109)	6 1
KCl · CaCl₂	600 (1112)	66 8	33 2	–	77 7 (139)	19	21	3 6-3 8 (.87-.92)	1 9-2.4 (.47-59)	2 10 (131)	1.69 (106)	5.3
KCl · CaCl₂	640 (1184)	29 2	70.8	–	68 3 (123)	.19	21	3.6-3.8 (.87-.92)	1.9-2.4 (.47-58)	2 13 (132)	1.90 (118)	4 8
KCl · NaCl	658 (1216)	56 1	43 9	–	98 9 (177)	23	24	3.6-3 8 (.87-92)	1 9-2 4 (.47-58)	2 06 (129)	1 53 (95)	6.7
K₂CO₃ · Na₂CO₃ · Ca₂CO₃	700 (1292)	48 1	29 9	22 0	74 6 (134)	28	.38	4.1 (1)	4 1 (1)	2 57 (158)	2 57 (156)	6 1
Na₂CO₃ · K₂CO₃	710 (1310)	49 2	50.8	–	61 0 (110)	.40	.37	4.12 (1.0)	4 12 (1 0)	2.48 (165)	1.94 (121)	5.8
CaCl₂	772 (1422)	100	–	–	61.1 (110)	19	.21	3.6-3.8 (.87-.92)	1.9-2.4 (.47-58)	2.15 (134)	2.07 (129)	4.3
KCl	776 (1429)	100	--	–	75 3 (135 5)	20	.21	3.6 (.87)	1.9-2.4 (.47-.59)	2.07 (129)	1.50 (94)	5.1
NaCl	801 (1474)	100	–	–	115.2 (207)	28	27	3.6 (.92)	1.9-2 4 (.47-58)	2 17 (135)	1.58 (97)	8.2
Na₂CO₃	851 (1564)	100	–	–	66 (119)	27	40	4.36 (1.06)	4.36 (1 06)	2.53 (158)	1 97 (123)	5 5
K₂CO₃	891 (1636)	100	–	–	56 4 (101)	22	36	4 1 (1)	4.1 (1)	2 43 (152)	1 90 (118)	5.0
Na F	988 (1810)	100	–	–	188.6 (339)	36	.39	10-19 (2.4-4.8)	10.7 (2.60)	2.56 (160)	1 95 (121)	15.9
Ca CO₃	1339 (2442)	100	–	–	126.9 (228)	.38	38	1.3 (.31)	1.3 (.31)	2.93 (183)	2.83 (183)	12.2
Ca F₂	1380 (2480)	100	–	–	90.9 (164)	38	.30	10-19 (2.4-1.8)	10.7 (2.60)	3 18 (198)	2 54 (159)	8.5

1767-006(T)

Figure 3-4 Candidate Salts for Advanced Solar Power Plant Applications

possible. Further, it was felt that traces of Na_2SO_4 could be troublesome, especially if it were to separate from the bulk mass and collect in one location. In addition, removal of Al oxides, K_2SO_4, $KClO_3$, Hg metal, and Mg $(OH)_2$ traces might be required. Figure 3-5 summarizes the suggested salt purification requirements.

SALT	SUPPLIER	OBJECTIONABLE IMPURITIES TO BE REMOVED		REQUIRED PROTECTIVE GAS ATMOSPHERE
$NaNO_2$				
$NaNO_3$		Na_2SO_4		
KNO_3	CROTON	AL OXIDES		N_2
KCI				
$Ca(NO_3)_2$			ALL TRACES OF WATER AND OXYGEN	
NaOH	HOOKER	Na_2SO_4		H_2
NaCl	MORTON			N_2
KOH	IMC	K_2SO_4, $KClO_3$, Hg		H_2
$MgCl_2$ (A,B)	DOW	$Mg(OH)_2$		
$CaCl_2$ (B)		?		N_2
$BaCl_2$ (C)	?	?		

(A) $MgCl_2$ "FLAKE" IS IN FACT: $MgCl_2 \cdot 6H_2O$ (ABOUT + 50% WATER)
(B) PURITY SPECIFICATIONS NOT DETAILED SUFFICIENTLY
(C) SUPPLIER AND PURITY NOT IDENTIFIED

1767-007(T)

Figure 3-5 Suggested Salt Purification Requirements

The removal of traces of water and oxygen should be done after the salt has been placed in the TES heat exchanger so that contact with the atmosphere will not occur after purification. The cost of fuel oil to heat the salt for drying would be only 2/3¢/lb at 80¢/gal of oil. Other costs are difficult to estimate. The need for a vacuum freeze/thaw purification cycle might design the thickness of the TES heat exchanger walls for certain configurations, thus increasing the unit cost. Alternately, a larger vacuum shell could be constructed to hold the heat exchanger so that only one very heavy walled unit would be required which could purify many units. The procedure to remove solid impurities ($NaSO_4$, primarily) is best conducted in aqueous solutions of the parent salt by selected chemical reactions. This would indicate that solid purification might best be undertaken by the salt manufacturer.

Figure 3-6 presents bulk (truckload lists) salt costs and an estimate of purified salt costs for each of the constituent elements of the eutectics listed in Figure 3-3. A significant increase in demand for TES applications could result in a cost reduction. In

	MANUFACTURERS TRUCKLOAD 20,000 LB	QUANTITY COST CORRECTED FOR WATER CONTENT	TOTAL COST INCL. $.05/LB FOR WATER, O_2, AND SOLID IM-PURITIES REMOVED
$MgCl_2, 6 H_2O$	.0850	.170	.22
$CaCl_2 (20\%) H_2O$	.0440	.055	.105
NaCl	.0177	--	.07
KCl	.0755	--	.1255
$NaNO_2$	.3095	---	.3595
$NaNO_3$	.1095	--	.1595
KNO_3	.1825	--	.2350
NaOH	.143	---	.193
KOH	.22	--	.27
$BaCl_2$	.155	---	.205

1767-008(T)

Figure 3-6 Cost Estimates, Individual Salts ($/lb), 1977 Prices

the other direction, prices will increase due to added purification costs as just discussed.
In two extreme cases ($MgCl_2$ and $CaCl_2$), crystalline water accounts for 50% and 20% of
the salt weight respectively so that in order to get 1 lb of $MgCl_2$, 2 lbm of $MgCl_2$
crystals must be purchased; this effectively doubles the cost of this salt even without
including the cost of water removal. The purchase price adjusted for water content is
shown in Column 2. The total estimated salt cost shown in Column 3 includes an
allowance of $0.05/lb on all salts for the energy required for water removal, the
amortization of a vacuum vessel and pumping station for vacuum bakeout, and
provisions for some extra supplier charge for solid impurity removal.

Using these cost figures, eutectic material ($/lb) and thermal storage ($/kWh$_t$)
costs can be computed based on the component weight breakdown. This information is
presented in Figure 3-7 for each of the eutectics, or single salts listed in Figure 3-3.

3.3   RECOMMENDATION

The salt selected as the principal one for this study was 20.5 KCl • 24.5 NaCl•
55.0 $MgCl_2$ which melts at 385°C (725°F). This salt is representative of chloride
systems, which are expected to be important in moderate to high temperature TES
applications. Reference 8 gives unusually detailed containment information indicating low
corrosion and specifying purification techniques. The thermal properties of the salt are
very good, much better than for hydroxides or nitrates, and it is neither toxic, caustic,
or oxidizing. The required constituent salts are inexpensive and readily available in

SALT ELEMENT A·B·C	MELT POINT °C(°F)	$/LB		$/KWht	
		BULK	INCLUDING PURIFICATION	BULK	INCLUDING PURIFICATION
$NaNO_3 \cdot NaOH$	246(475)	.115	.165	5.13	7.36
$NaCl \cdot NaNO_3$	297(567)	.105	.155	4.27	6.30
$NaNO_3$	307(585)	.11	.16	4.81	6.99
$NaOH$	318(605)	.143	.198	3.59	4.84
$KCl \cdot KNO_3$	320(608)	.178	.230	12.93	16.7
KOH	360(680)	.22	.27	13.04	16.0
$KCl \cdot NaCl \cdot MgCl_2$	385(725)	.069	.173	1.20	3.00
$NaCl \cdot BaCl_2 \cdot MgCl_2$	418(784)	.088	.172	2.06	4.02
$NaCl \cdot MgCl_2$	450(842)	.045	.13	0.77	2.23
$CaCl_2 \cdot KCl \cdot NaCl$	465(869)	.038	.096	0.93	2.36
$NaCl \cdot CaCl_2$	500(928)	.035	.093	0.99	2.63
$KCl \cdot NaCl \cdot CaCl_2$	504(939)	.029	.096	0.83	2.73

1767-009(T)   **Figure 3-7 Cost of Candidate Salts and Salt Eutectics, 1977 Prices**

large quantities. Some possible drawbacks are that this salt does have relatively large volume change on fusion and that $MgCl_2$ tends to form a hydrate $MgCl_2 \bullet 6H_2O$ if the anhydrous salt is exposed to moist air. However, these are not serious from the viewpoint of overall system operation. Proper container design can accommodate the density change and demonstrated purification techniques can remove all significant traces of water.

The other salts which were recommended as alternatives for this test program are KOH and $NaNO_3$. Because they melt at distinctly lower temperatures (360°C for KOH and 307°C for $NaNO_3$), in an actual system these salts could be used in combination with a chloride eutectic to cover the entire temperature range of interest for feedwater heating, boiling, and superheating. Hydroxides and nitrates are already in use as heat transfer and storage media. While neither of these salts has thermal properties that compare with chloride salts, they have other advantages, particularly for the temperature range of interest. Specifically the ability of $NaNO_3$ to passivate steels could be important in active designs where slight atmospheric contamination of the salt is possible.

No problems regarding long-term stability or kinetics of transformation are expected with any of these salts. Vapor pressures for all the salts are low at the temperatures of interest, which simplifies containment vessel construction. Supercooling does occur with some chloride salts (particularly $ZnCl_2$); however, it is not expected to occur with the specific eutectic chosen.

3-12

4.0 IDENTIFICATION OF HEAT EXCHANGE CONCEPTS

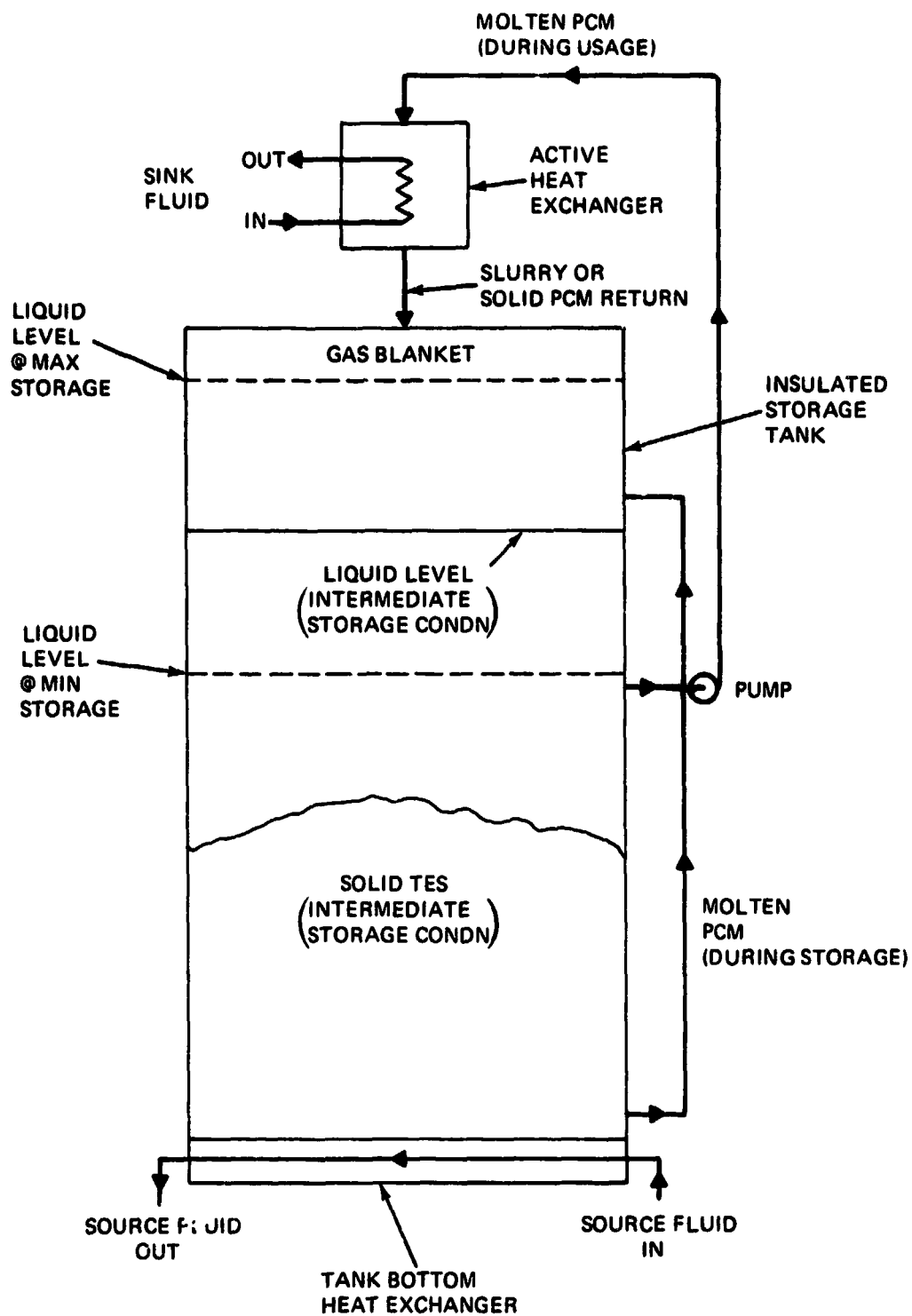### 4.1 OVERALL SYSTEM CONSIDERATIONS

The active heat exchange concept lends itself to a variety of overall system flow arrangements. For discussion purposes, it is convenient to consider five basic flow schematics, each of which has some variants:

- Single-tank pumped fluid system (Figure 4-1)
- Two-tank pumped fluid system (Figure 4-2)
- Multiple-tank pumped fluid system (Figure 4-3)
- Natural convection system (Figure 4-4)
- Intermediate liquid metal loop (Figure 4-5).

Each component takes advantage of the higher density for the solid compared with the liquid. The solid is forced by gravity against the bottom of the tank where it can be melted by hot source fluid during the energy storage mode of the cycle. For schematic purposes, the active heat exchangers for the pumped systems are shown as separate units located at the top of the storage tanks. Many of the active heat exchanger concepts require a location within the tanks (though near the top), and, in some cases, a location beneath the free liquid surface of the molten salt.

The active heat exchange concepts are discussed under three generic categories (mechanical scrapers, vibrators and mixed fluid streams) which include the following specific concepts:

- Translating scrapers
- Rotating scrapers
- Rotating drum with fixed scraper
- Mechanical vibrators
- Ultrasonic liquid bath
- Tube flexing
- Gas bubble turbulation
- Direct contact heat exchange.

Figure 4-1 Single Tank Pumped Fluid System Schematic

1767-010(T)

SINK
FLUID

OUT

IN

ACTIVE
HEAT EXCHANGER

MOLTEN PCM
(USAGE)

SOLID
PCM
STORAGE
TANK

OPTIONAL LIQUID
SUPERHEAT H/X

TANK BOTTOM
HEAT EXCHANGER

MOLTEN PCM (STORAGE)

OUT

IN

SOURCE
FLUID

LIQUID
PCM
STORAGE
TANK
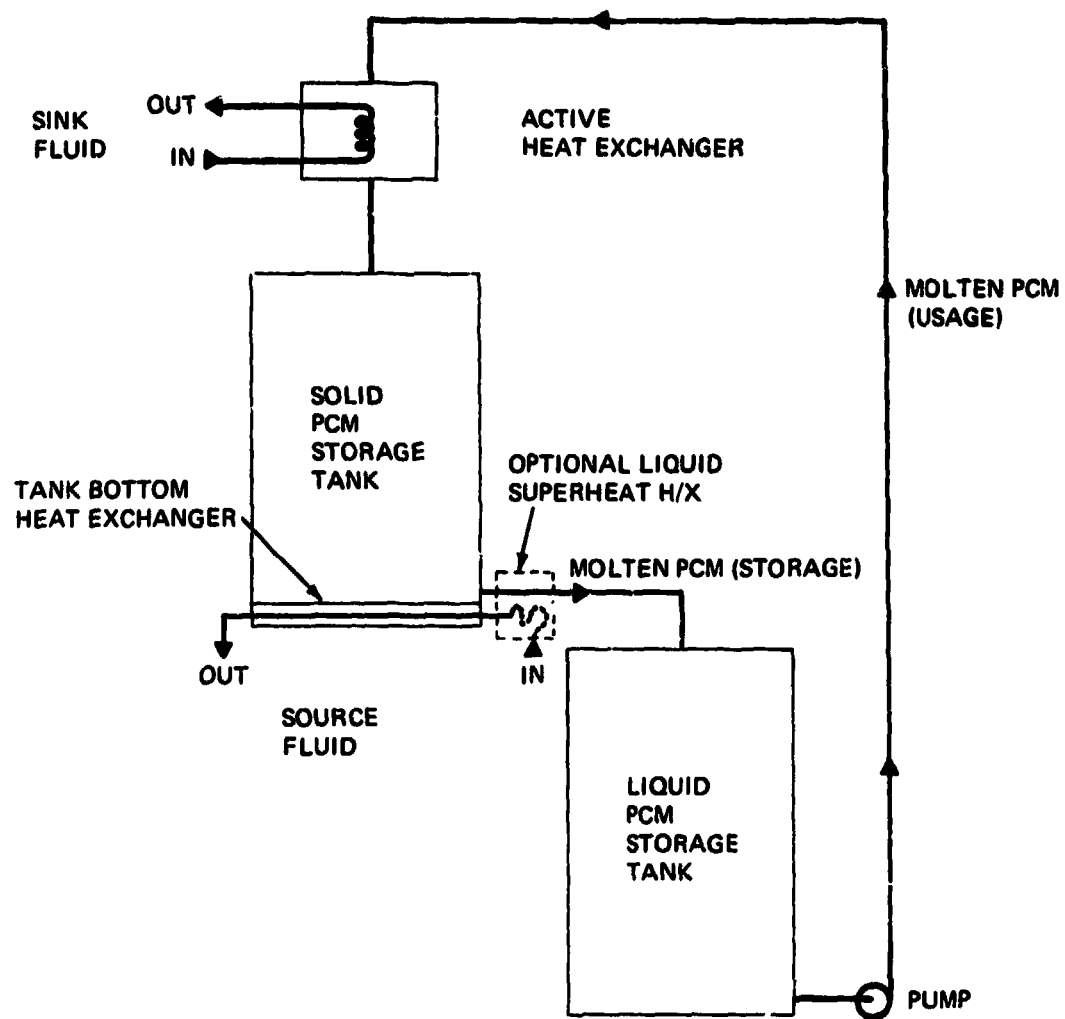
PUMP

1767-C11(T)

Figure 4-2 Two - Tank Pumped Fluid System Schematic
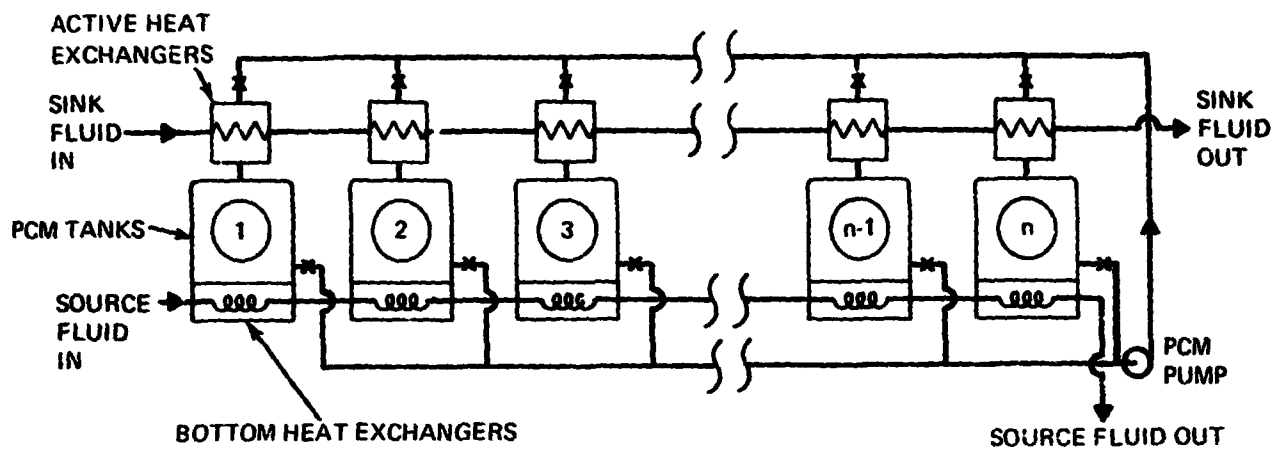
1767-012(T)

Figure 4-3 Multiple - Tank Pumped Fluid System Schematic

1767-013(T)

Figure 4-4 Single - Tank Natural Convection System Schematic

Figure 4-5 Two - Tank Liquid Metal Carrier System Schematic

1767-014(T)

The applicability of these concepts to the overall system flow arrangements is shown in Figure 4-6.

It should be mentioned that corrosion in flowing salt systems may be more severe than in passive designs where the salt is essentially immobile. According to Reference 14, in a flowing salt system thermal potentials exist which cause the removal of metal at hot points and its subsequent deposition at cooler sections.

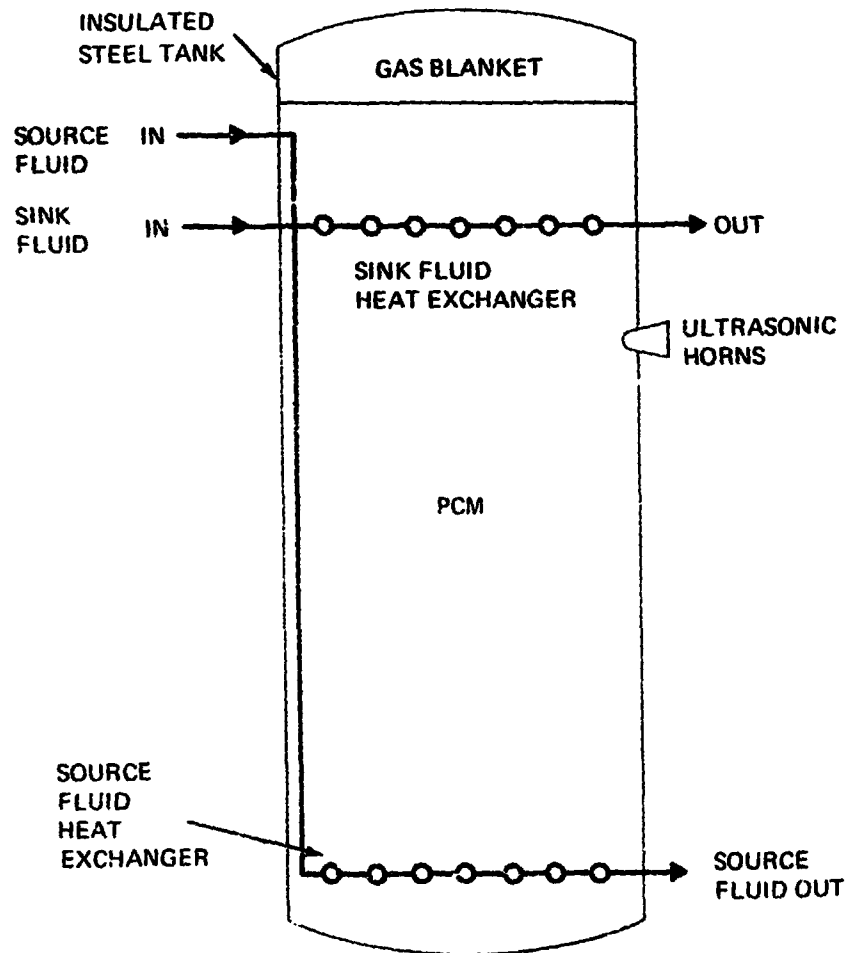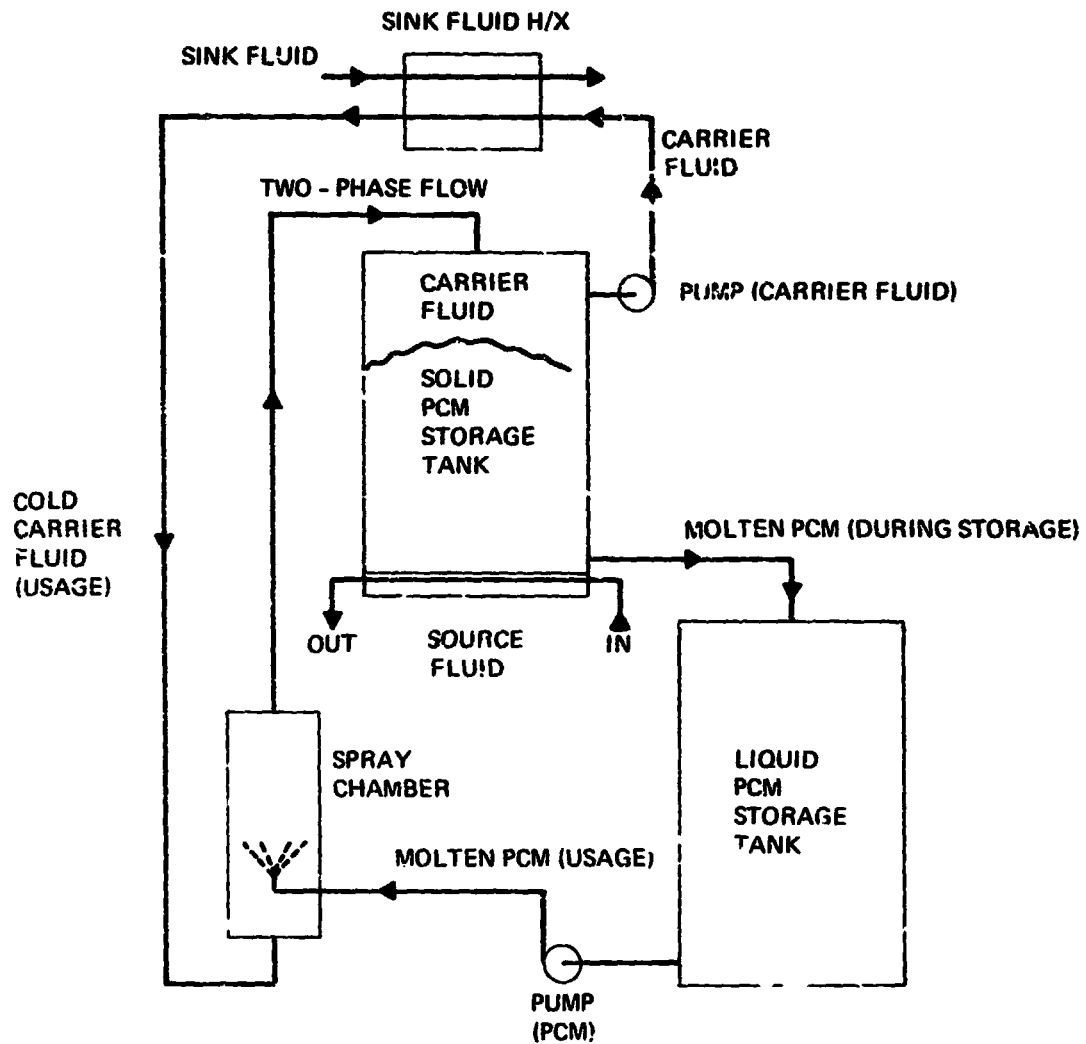| HEAT EXCHANGER CONCEPT — SYSTEM CONCEPT	TRANSLATING SCRAPER	ROTATING SCRAPER	ROTATING DRUM	MECHANICAL VIBRATOR	ULTRASONIC LIQUID BATH	FLEXIBLE TUBES WITH PRESSURE PULSATIONS	DIRECT CONTACT HEAT EXCHANGE	GAS BUBBLE TURBULATION
SINGLE TANK PUMPED SYSTEM		x	x					x
TWO TANK PUMPED SYSTEM			x					
MULTIPLE TANK PUMPED SYSTEM		x	x					x
NATURAL CONVECTION TANKS	x	x		x	x	x		
INTERMEDIATE LIQUID METAL LOOP	x	x	x	x	x	x	x	x

1767-015(T)

Figure 4-6. Active Heat Exhanger - System Flow Combinations

4.1.1 Pumped Single-Tank System

In the pumped single-tank concepts (Figure 4-1) the solidified PCM is essentially at the phase change temperature within the storage tank. Even if an active heat exchanger were to extract sensible energy from the solid before returning it to the tank, heat transfer with the liquid at the top of the tank would bring the solid back to phase change temperature. During the thermal storage cycle, it would be possible to get some sensible storage in the liquid, because liquid hotter than the phase change temperature could be collected at the bottom side heat exchanger and fed to the top of the tank. Having lower density, it would tend to remain there, thermally stratified, though cooling slowly by conduction heat transfer to the cooler PCM located lower in the tank. The liquid super-heat would be quickly eliminated during the usage period by agitation of the liquid and by remelting of the solidified PCM sinking through it.

Elimination of the liquid superheat will reduce the temperature difference available to the active heat exchanger, and this will increase the size of the heat exchanger somewhat.

4-6

The single tank system has an advantage, however, in being able to accept either a partially solidified slurry or a wholly solidified PCM returning from the active heat exchanger. A single tank may, because of lower surface to volume ratio, be cheaper to build and insulate for a given level of heat loss to the environment. The concept is adaptable to multiple smaller tanks in parallel, however, if the economics of a particular application favored such an approach.

4.1.2 Pumped Double-Tank System

Use of the two tanks (Figure 4-2) permits the system to use the sensible heat storage capacity of the PCM in addition to the heat of fusion. This could reduce the amount of PCM required by as much as 30%, with a corresponding reduction in the volume of each of the tanks. Allowing for the higher density of the solid, the combined two-tank volume might be only 20-40% greater than the single-tank system. To take advantage of solid sensible storage capacity, however, the active heat exchanger would have to be a type which provides a completely solidified return (e.g. , a rotating drum rather than an internal scraper). The flow of the molten PCM from the tank bottom heat exchanger to the liquid storage tank could be by gravity, if the liquid storage tank were located beneath it, or a pump (not shown) could be used. In addition, depending on the thermodynamics of the application, a heat exchanger might be used to further superheat the liquid before it enters the liquid storage tank.

4.1.3 Multiple-Tank Pumped Fluid System

The multiple-tank system(Figure 4-3) is thermodynamically equivalent to the two-tank system in permitting use of sensible as well as latent heat thermal storage. The system is based on the "one tank empty" concept, for which n-1 tanks are sized to hold all the PCM at the hottest liquid temperature, and one additional tank is provided for transfer operations. The total volume of all the tanks is then only n/(n-1) of the required liquid volume. For example, an 11-tank system with 30% sensible storage would require only 70% of the PCM and 77% of the total volume of a comparable single-tank system.

With the system shown in Figure 4-3, PCM is transferred from one tank to another during the usage part of the cycle, but stays within the tank it is in for the storage part of the cycle. The system has valves on the PCM lines, but does not require valves for the high pressure source and sink fluid lines. The source fluid enters at Tank 1, which would tend to melt first, followed by the others in sequence.

The multiple-tank system advantages of smaller total tank volume and PCM mass are to some extent offset by the complexity of the PCM flow control system and additional PCM piping and valves (which must be heat jacketed to prevent freezing).

4.1.4 Single-Tank Natural Convection System

In this system, both the storage and usage heat exchangers are located within the PCM storage tank (Figure 4-4). Solidified PCM is removed from the usage heat exchanger (located at the top of the tank) by ultrasonic vibrations in the liquid and settles under gravity to the bottom of the tank. Alternatively, the heat exchanger surfaces might be mechanically vibrated, flexed or scraped to remove the solid. A vertical leg is provided within the tank for the source fluid inlet line. By locally melting the solid PCM this assures a liquid relief path to accommodate the volumetric expansion associated with melting.

This system is relatively simple compared with the pumped fluid systems, but requires some preliminary experiments to establish relationships between vibration frequencies, amplitudes, and solid layer buildup prior to removal. If the solidification thickness can be kept to the same level as the pumped scraper systems (or smaller), this system would have performance equivalent to the single-tank pumped system. By keeping the PCM in the tank, it may be possible to build and fill the tank in a factory, and ship sealed units to the site, permitting better control of salt purification processes.

4.1.5 Two-Tank Liquid Carrier Systems

One such system uses an intermediate liquid metal loop to transfer heat from the molten PCM to the sink fluid (Figure 4-5). The active heat exchanger is replaced by a chamber in which molten PCM is sprayed into a flowing liquid metal stream which is colder than the PCM melt temperature. The droplets of PCM solidify, heating the liquid metal stream, as they are carried by the liquid metal to the solid PCM storage tank. A liquid metal to sink fluid heat exchanger would still be required, but this would be simpler than an active heat exchanger for PCM. Thermodynamic losses associated with an intermediate loop could be kept small for this system, because liquid metals have good heat transfer characteristics and because the use of small PCM droplets gives very little temperature difference between the solidified PCM and the carrier fluid in the two phase flow entering the solid PCM storage tank.

This concept is limited to those combinations of salt and carrier fluid that are both nonreactive and immiscible with each other. The droplet freezing and transport requirements are straightforward and technology is available for all components of the liquid metal loop.

The liquid metal loop is also attractive for all of the active heat exchanger concepts, for both safety and performance considerations. Leaks in the active heat exchanger should be much less of a hazard with a low pressure liquid metal sink fluid than with high-pressure water. Also, the low pressure of the liquid metal would permit thinner heat exchanger wall thicknesses, with correspondingly higher heat flux values. The wall thermal resistance is the dominant resistance in many of the active systems. There would still have to be thick walls for the liquid metal to water heat exchangers, but these would be passive, rather than active, units.

4.2   ACTIVE HEAT EXCHANGER CONCEPTS

Active heat exchangers can be made with a wide variation of geometric and mechanical design configurations. After a preliminary screening, each of the concepts presented below were judged technically feasible and worthy of more detailed evaluation.

- Tube-shell heat exchanger with translating multiple tube scraper

- Rotating scrapers

- Rotating drum with fixed scraper

- Mechanical vibrators

- Ultrasonic liquid bath

- Flexible tubes with pressure pulsations

- Liquid bath with gas bubble turbulation

- PCM spray with intermediate liquid metal loop (direct contact heat exchange).

Also, some of the concepts (scrapers, vibrators, ultrasonic bath, flexible tubes) may be significantly improved by nonstick coatings. Teflon could be used for service temperatures less than 260°C (500°F) and highly polished nickel plated coatings for higher

temperatures of 650°C (1200°F). The scraper concepts could also be improved by the use of thermal conductivity enhancers. Any of the first seven concepts can transfer heat directly with the utility heat sink fluid (high pressure steam or water) or they can be designed with an intermediate heat transport loop which uses a low pressure fluid (e.g., liquid metal).

4.2.1 Tube Shell with Translating Scraper

This concept, illustrated schematically in Figure 4-7, bears the closest resemblance to the passive tube shell heat exchanger of Reference 1. The addition of a motor-driven scraper plate, translating longitudinally over the cylindrical length of the shell, would permit using fewer tubes.
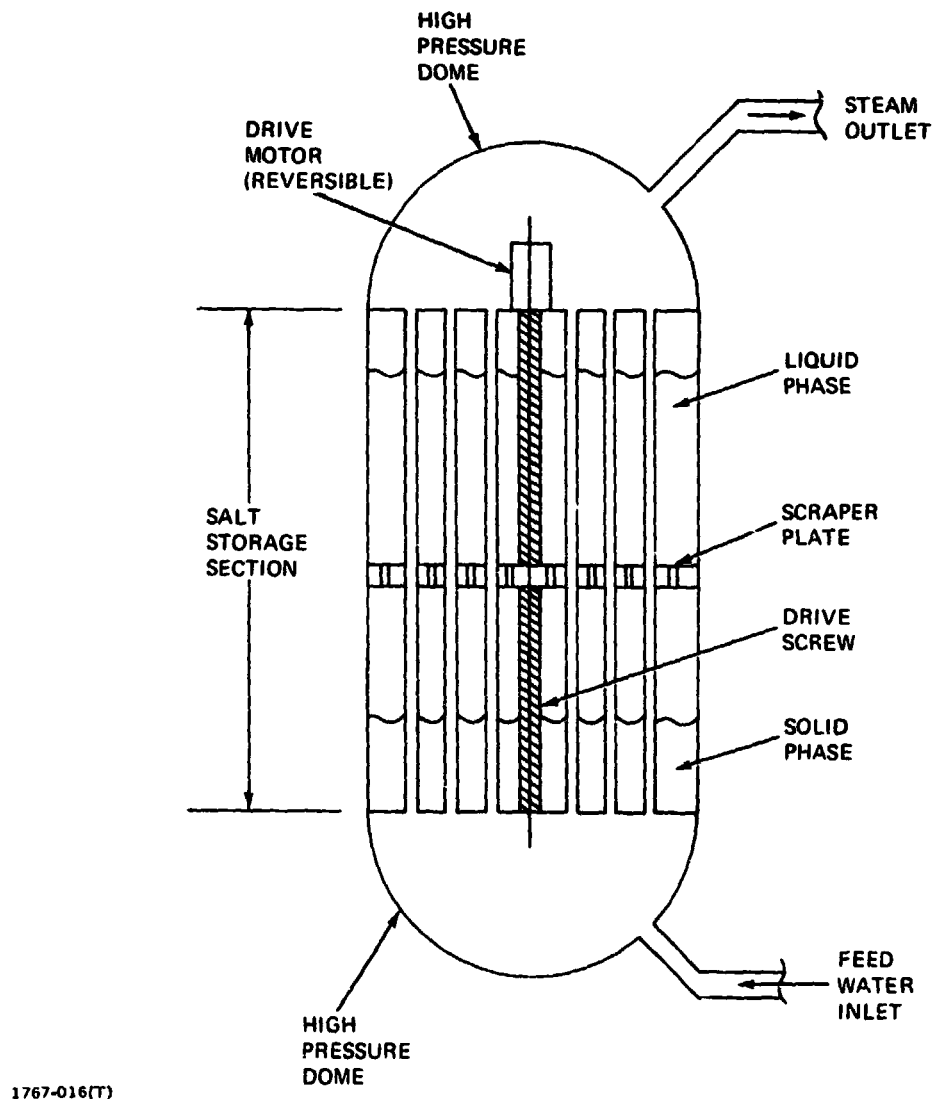

1767-016(T)

Figure 4-7 Proposed Heat Exchanger with Multiple - Tube Translating Scraper
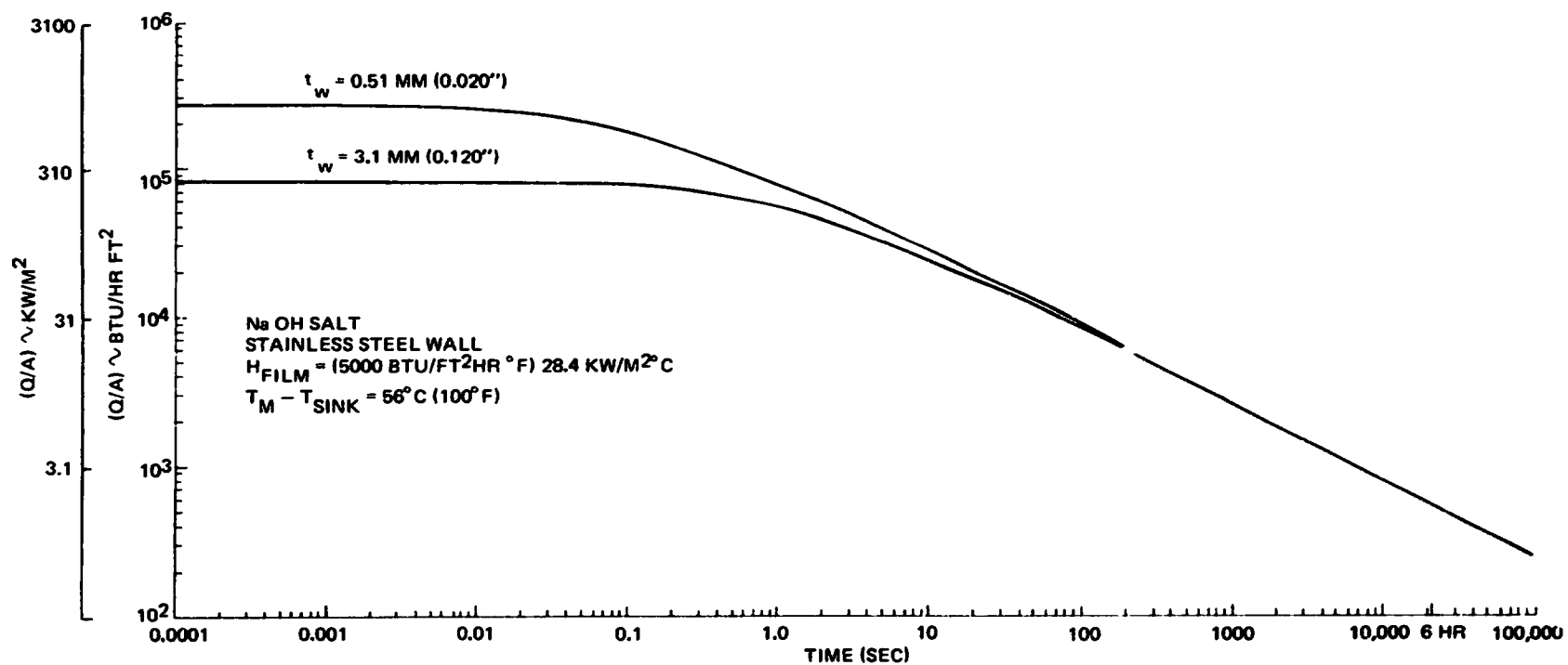
For example, assuming the same NaOH storage conditions a static tube/shell heat exchanger would have a mean heat flux of approximately 4098 W/M^2 (1300 Btu/hr/sq ft) of tube external area allowing for cylindrical heat conduction and a 6-hr freezing period As seen in Figure 4-8, this could be increased by a factor of seven using a scraper plate traversing the length of shell once every 100 sec. The screw drive shown is strictly schematic and could be replaced by a variety of other actuators.

Reducing the number of tubes by a factor of seven would also reduce the size of the domes almost in proportion (the domes need not have the same diameter as the shell). The use of a scraper plate should permit some flexibility in tube location because there will now be some circulation of PCM within the shell. The scraper plate motion would be adjusted as needed to allow for variations in the PCM solid fraction. It may be possible to locate the tubes to permit the scraper plate size to be only a small fraction of the shell cross-sectional area, though the system would still be somewhat cumbersome compared with other mechanical systems.

4.2.2   Rotating Scrapers

Rotating scrapers may be of either the internal or external scraped surface type, (Figures 4-9 and 4-10, respectively). In either case, the scraper is located directly in the PCM flow passage, and the scraper blades serve a dual function in acting as an impeller to circulate the PCM. The scraper units could be located within the liquid in a single tank storage system or connected to the tank with piping. With both arrangements the tank would be sized to permit some remaining liquid PCM at the end of the usage cycle. The PCM would not fully solidify in passing through the scraper unit and would be discharged as a slurry. The solid fraction in the slurry would settle out due to density differences, so that relatively pure liquid would be available higher up in the tank.

A variety of drive options are available for the scraper. Figure 4-9 shows the motor external to the tank, with a rotary seal where the drive shaft penetrates the tank wall. With only minor mechanical complications, the penetration could be located above the free liquid surface, in the region of the inert gas blanket. An alternative arrangement is to locate the motor within the tank, eliminating the seal entirely, providing the motor can be adequately cooled.

1767-017(T)

Figure 4-8 Mean One-Dimensional Heat Flux Versus Solidified Salt Residence Time

BLADES TO
BE MOUNTED
TO DRIVE SHAFT
SO ROTATION
PUMPS SALT
SLURRY

DIRECTION
OF ROTATION
OF SCRAPER
BLADES

LOW
PRESSURE
SALT

SALT
STORAGE
TANK

HIGH
PRESSURE
STEAM

LOWER
HEAT EXCHANGER

SCRAPER
BLADES

FEED
WATER
INPUT

STEAM
OUTPUT

LIQUID

SOLID

ROTARY SEAL

SCRAPER
DRIVE MOTOR
(IF DRIVE CAN
BE IN TANK SEAL
CAN BE ELIMINATED)

LOW PRESSURE
SALT STORAGE
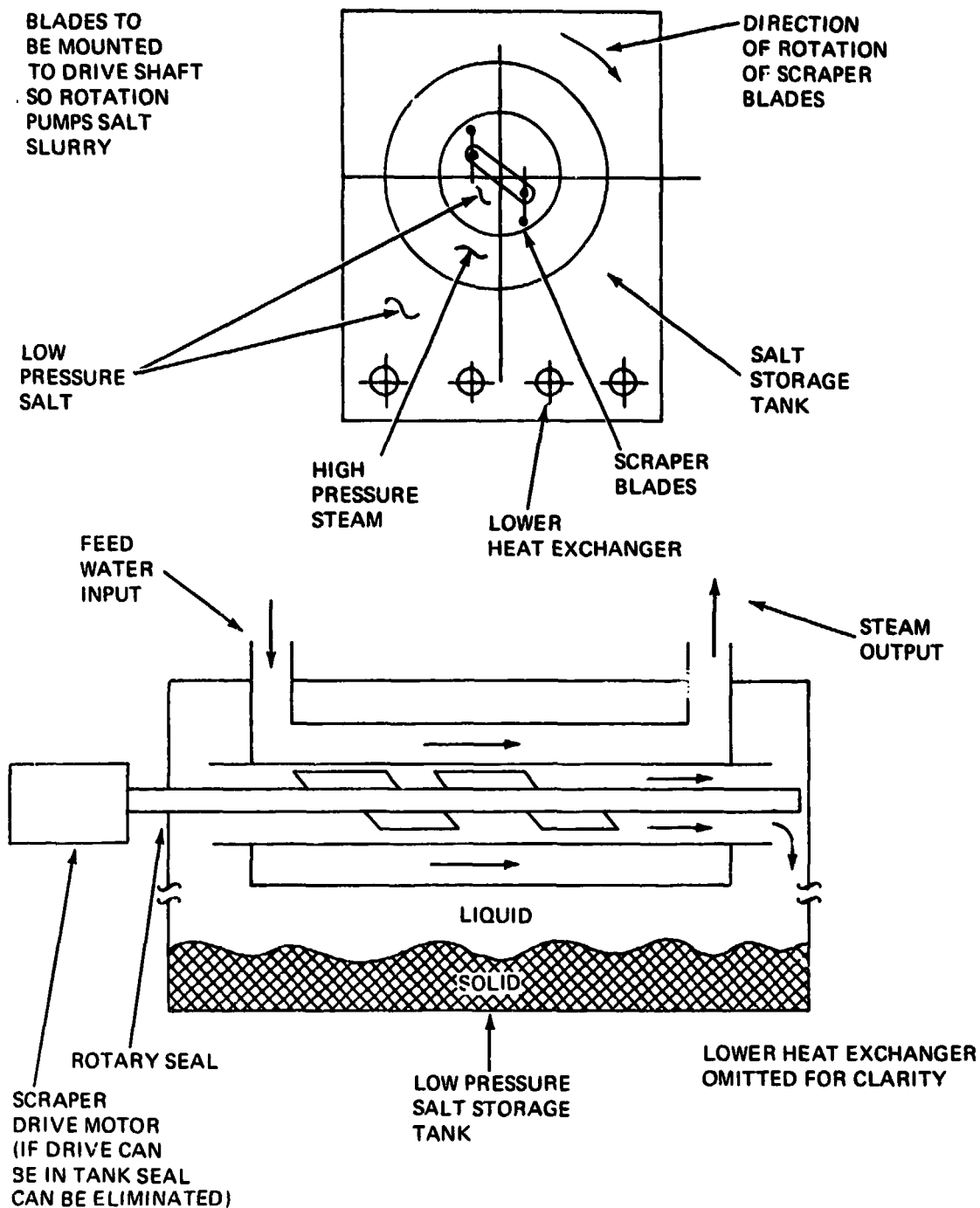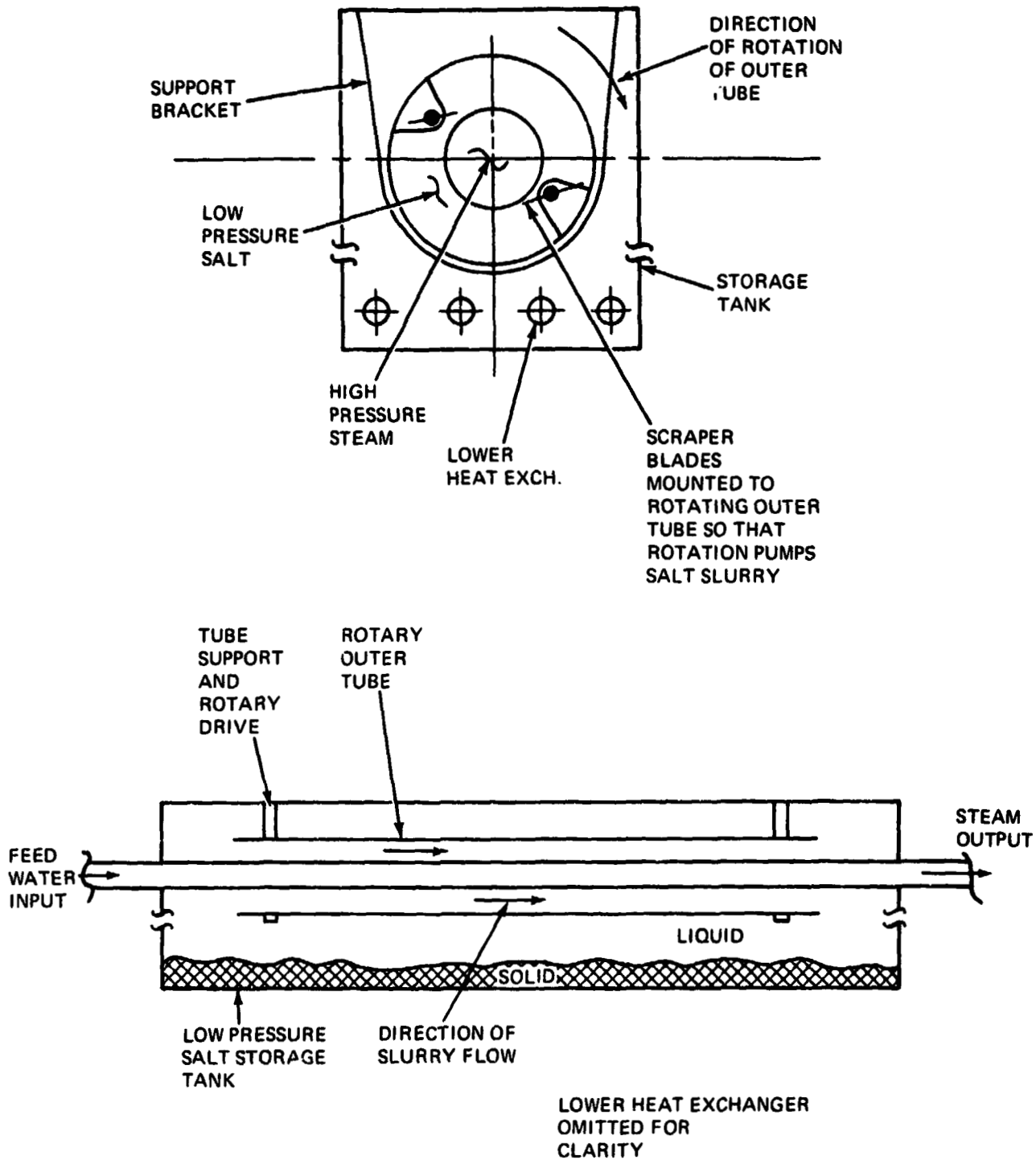TANK

LOWER HEAT EXCHANGER
OMITTED FOR CLARITY

Figure 4-9 Proposed Heat Exchanger Internal Tube Scraper

4-13

Figure 4-10 Proposed Heat Exchanger External Tube Scraper

1767-019(T)

The internal scraper is similar to that used in the food industry. In its simplest form, the high-pressure sink fluid flows in the concentric annular passage surrounding the PCM tube. For 16.5 mPa (2400 psi) sink fluid pressure, 344°C (650°F) design temperature, with stainless steel, the minimum wall thickness-to-radius ratio is approximately 0.15, permitting a 3.1 mm (0.120-in.) wall thickness with a 38.1 mm (1.5-in.) tube diameter. This is the same wall thickness as used in Figure 4-8, and, taking those conditions as an example, the scraper heat exchanger would, with liquid PCM passing through it, have a heat flux of 246 kW/m^2 (78,000 Btu/hr ft^2) if the surfaces were scraped every 0.1 sec. This would require a rotational speed of 600 RPM for a single-bladed scraper or 300 RPM for a double-bladed scraper.

A somewhat more complicated construction (Figure 4-11) passes the high-pressure sink fluid through many small-diameter, thin-walled tubes, arranged to form a cylindrical wall. (A configuration similar in some respects to that used in some regeneratively cooled liquid propellant rocket nozzles). Using 6.35 mm (0.250-in.) OD stainless steel tubes with 5.1 mm (0.20-in.) wall thickness, the heat flux (Figure 4-8) would be approximately 564 kW/m^2 (179,000 Btu/hr ft^2), which is more than twice the value for the

1767-020(T)
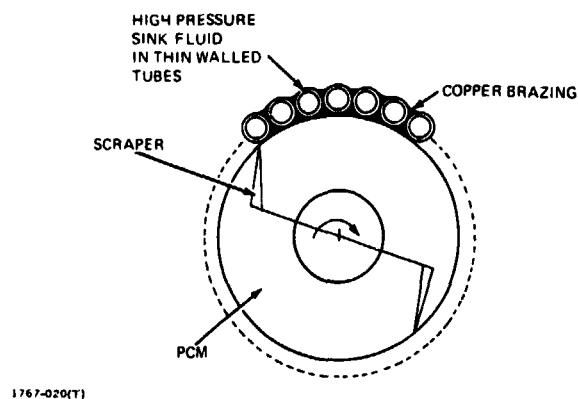
Figure 4-11 Rotating Internal Scraper Based on Thin-Walled Tubing

concentric annulus, for the same time interval (0.1 sec). To minimize thermal resistance, the space between tube OD and the scraped cylindrical surface is shown filled with copper, material compatibility considerations permitting. If necessary, a thin-walled inner steel liner might also be used. The tubes would be connected to manifolds at either end of the scraper. One advantage of this construction from a design standpoint is that the diameter of the scraped surface is no longer limited by wall thickness considerations. Larger diameters can be used, and this may be advantageous in full-scale applications.

Regardless of choice of construction, there will be some loss in performance as the PCM flows through the scraper due to build up of solid fraction in the PCM slurry. The loss is dependent on the distribution of the solid within the slurry, being least if the solid, once removed, can be kept away from the wall. For the case of initially pure liquid, gradually solidifying as a homogenous slurry, the reduction in mean heat flux can be estimated from the relation

$$\frac{\left(\overline{q/A}\right)}{\left(\overline{q/A}\right)_{\substack{pure \\ liquid}}} = \frac{1 - \gamma_{\ell,f}}{\left(1 - \frac{u_i}{u_f} + \frac{u_i}{2} \ell n \left[\left(\frac{2 + u_i}{2 + u_f}\right)\left(\frac{u_f}{u_i}\right)\right]\right)}$$

where

$$u_i = \sqrt{1 + \frac{2 q_o t}{B_o}} - 1$$

$$u_f = \sqrt{1 + \frac{2 q_o t}{B_o \gamma_{\ell,f}}} - 1$$

$$q_o = U (T_m - T_o)$$

$$B_o = L \rho_s k_s / U$$

$$U = \left[1/h + t_w/k_w\right]^{-1}$$

and $\gamma_{\ell,f}$ = liquid fraction in slurry at discharge

with

h = film coefficient

t_w = wall thickness

k_w = wall conductivity

k_s = solid PCM conductivity

L = heat of fusion

ρ_s = PCM solid density

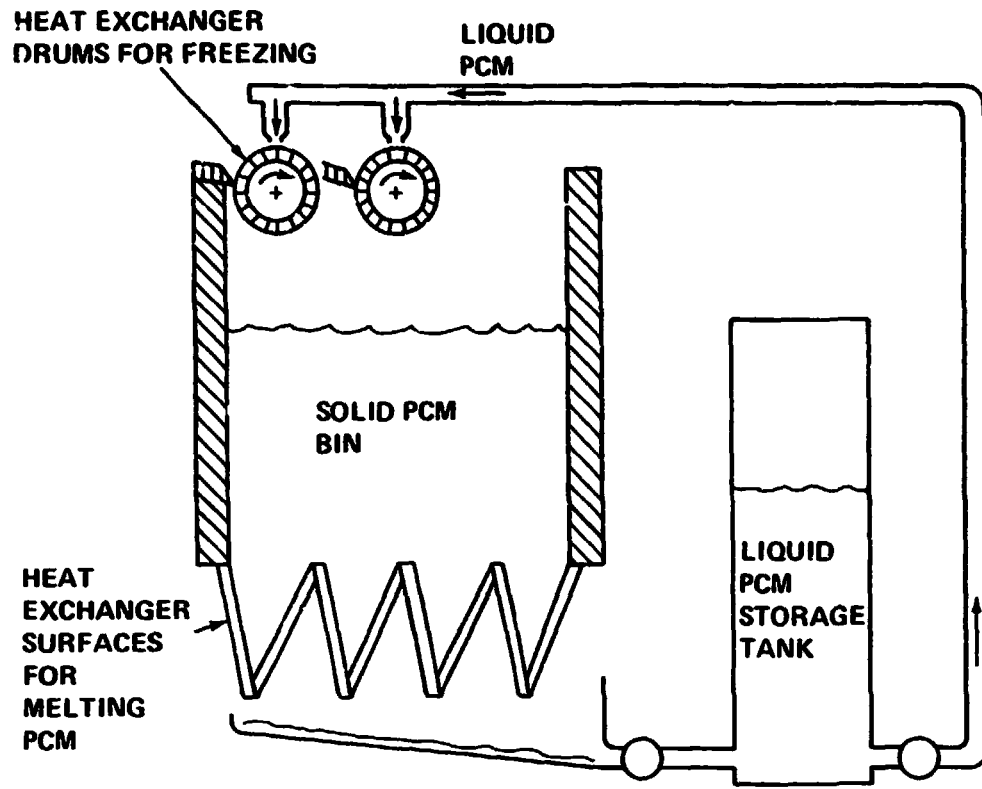T_o = sink fluid mean temperature

T_m = PCM melt temperature

For the 3.1-mm (0.120-in.) wall thickness condition calculated previously with (q/A) pure liquid = 246 kW/m^2 (78,000 Btu/hr ft^2), the mean heat transfer through the slurry would decrease only 7.5% with an exit liquid fraction of 0.10 (90% solid). The small falloff in performance is due to the small salt side thermal resistance compared with that of the relatively thick stainless steel wall. With the 0.51-mm (0.020-in.) wall thickness, by contrast, the falloff in performance would be 22%. The loss would be greater in both cases with lower RPM scrapers.

The concentric internal annulus scraper requires an outer tube which, because of increased radius, must be thicker than the inner tube. This adds to material cost but does not affect the heat transfer. The external scraper (Figure 4-10) puts the low-pressure PCM through the annulus and the high-pressure sink fluid through the inner tube. This eliminates one thick-walled piece and simplifies the high-pressure connections. This may be offset to some extent by mechanical considerations since the diameter of the rotating parts is larger, and centrifugal force tends to lift the scraper edge from the surface.

The development test article requires a minimum heat flux of 10 kW. For NaOH PCM, and the conditions previously described, this could be met by a 76.2-mm (3-in.) ID x 203.2-mm (8-in.) long scraped inner tube (using the multiple thin-walled tube construction), flowing PCM at a minimum rate of 126 kg/hr (277 lb/hr); flow velocity = 0.0046 m/sec (0.015 ft/sec). This would yield an exit slurry with 10% liquid. Higher flow rates could be used, with increasing liquid fraction in the exit slurry. The heat sink fluid passages would consist of approximately 40 tubes of 6.35-mm (0.25-in.) OD and 0.051-mm (0.020-in.) thickness taking high-pressure water flow at a velocity of 3.96 m/sec (13 ft/sec) for full simulation at the design film coefficient of 28.4 kW/m^2°C (5000 Btu/hr ft^2°F.) For safety during testing, the high-pressure water can be replaced by other fluids (Dow-A, Hitec, Liquid Metals) retaining thermal simulation by keeping the product of film coefficient and wall-to-fluid temperature difference constant.

4.2.3   Rotating Drum

The rotating drum scraper concept is shown in Figure 4-12. The fluid to be heated passes through an annular flow channel between the inner and outer tubes. Molten salt is sprayed on the outer tube surface where it solidifies as heat is transferred from it to the internal heat transport fluid. As the drum rotates, a fixed scraper blade continually removes the solid salt buildup.

HEAT EXCHANGER
DRUMS FOR FREEZING

LIQUID
PCM

SOLID PCM
BIN

HEAT
EXCHANGER
SURFACES
FOR
MELTING
PCM

LIQUID
PCM
STORAGE
TANK

716:-021(T)

Figure 4-12 Rotating Drum Concept

For the drum freezing process, the PCM thickness, δ , which can be frozen during rotation through an angle θ (less than 2π), at a rotational speed, Ω , neglecting sensible energy contributions and assuming one-dimensional heat transfer, may be approximated by the relation:

$$\delta = \frac{k_s}{U} \left[\sqrt{1 + \frac{B}{\Omega}} - 1 \right]$$

where

$$B = \frac{2U^2}{k_s} \frac{(T_m - \overline{T}_f)\theta}{\rho_s \,\Delta H_f}$$

and

$$\frac{1}{U} = \frac{1}{h} + \frac{t_w}{k_w}$$

4-18

with

h = sink fluid film coefficient

t_w = drum wall thickness

k_w = drum wall thermal conductivity

$\overline{T}_f$ = mean sink fluid temperature

The rate, $\dot{m}$, at which PCM can be frozen by an individual drum of length, L, and radius, R, is then

$$\dot{m} = \rho_s \, L \, R \, \Omega \, \delta$$

or

$$\dot{m} = \rho_s \, L \, R \frac{k_s}{U} \Omega \left[\sqrt{1 + \frac{B}{\Omega}} - 1 \right]$$

from which it can be seen that the mass freezing rate, $\dot{m}$, increases with Ω, approaching asymptotically, an upper limit

$$\dot{m}_{\Omega \to \alpha} = \rho_s \, L \, R \frac{k_s}{U} \frac{B}{2} = \frac{L \, R \, U \left(T_m - \overline{T}_f \right) \theta}{\Delta H_f}$$

Clearly high values of U and θ are desirable. Adhesion of the salt PCM to the drum surface should not present a problem. Indeed, some surface treatment to lessen the adhesion would be needed to minimize scraper power requirements.

To obtain high values of U, high values of h and a relatively thin wall, t_w, are needed. This can be accomplished by putting the sink fluid through multiple passages adjacent to the drum surface, using many stiffening ribs. Alternatively, multiple small-diameter tubes, similar to that discussed for the rotating scraper, could also be used. The drum diameter will be somewhat larger than the scraper surface of a rotating scraper, however, so that more (or larger diameter) tubes would be required. For the rib stiffened construction, the drum surface will tend to bulge outward between the ribs, if a high pressure sink fluid is used. This requires a sufficiently stiff design to insure a relatively thin and uniform salt layer.

4-19

A major mechanical difference between this concept and the rotating scraper is the need for two high-pressure water side seals for each rotating drum. Because water leakage cannot be permitted to contaminate the PCM, the seals would have to be of the gas pressurized type. The gas would be the same as that used for the inert blanket above the PCM. The gas would leak into both the PCM blanket and the water circuit. The gas leakage rates would have to be small, and gas in the water circuits would ultimately have to be removed from the steam condenser by the deaerator already present. The importance of any seal leakage problem can be minimized if the concept is used in conjunction with an intermediate low pressure heat transport loop.
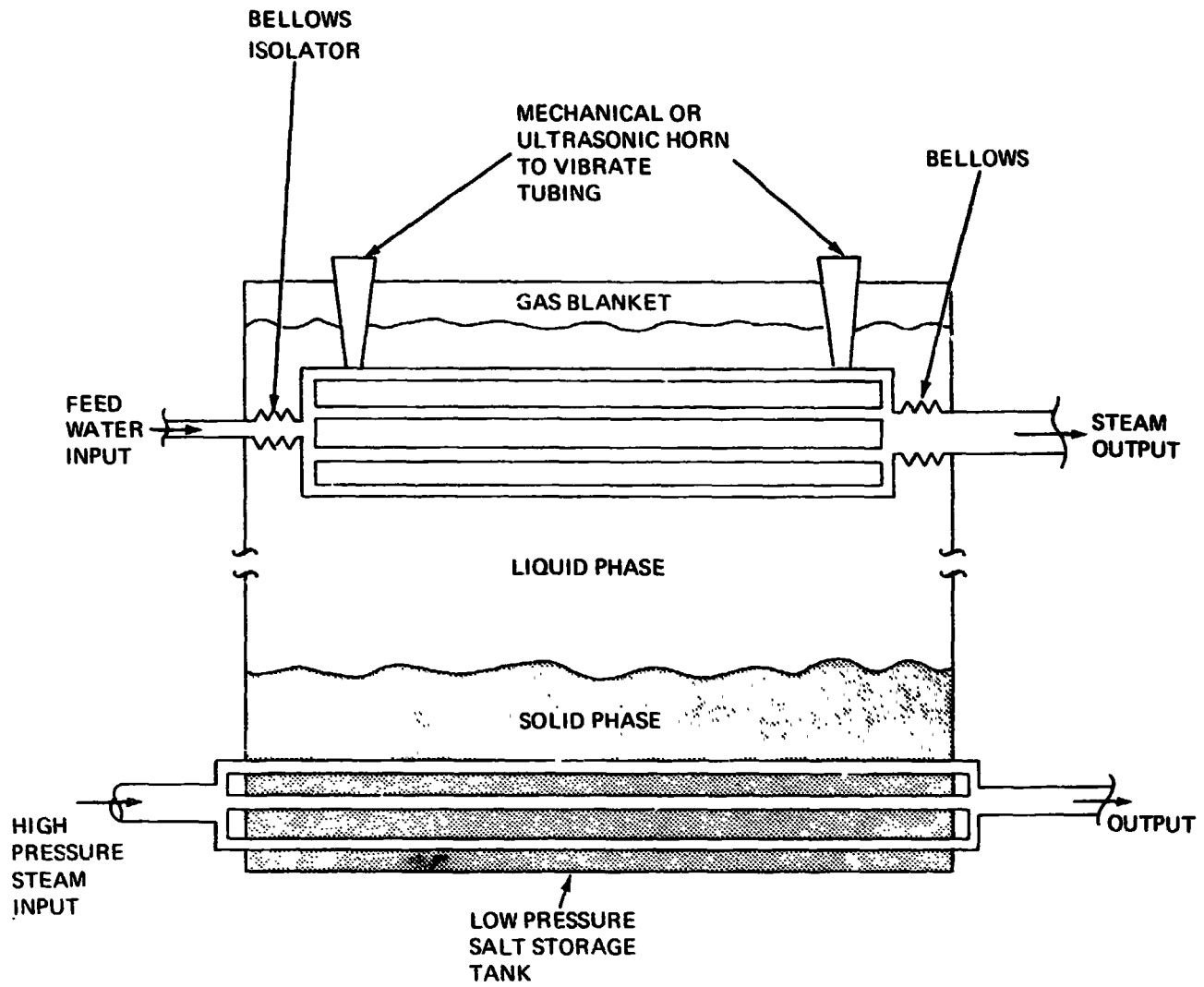
The major advantage of the rotating drum compared with the rotating scrapers is the capability of discharging subcooled solid rather than partially solidified slurry, hence increasing the specific heat storage capacity of the PCM.
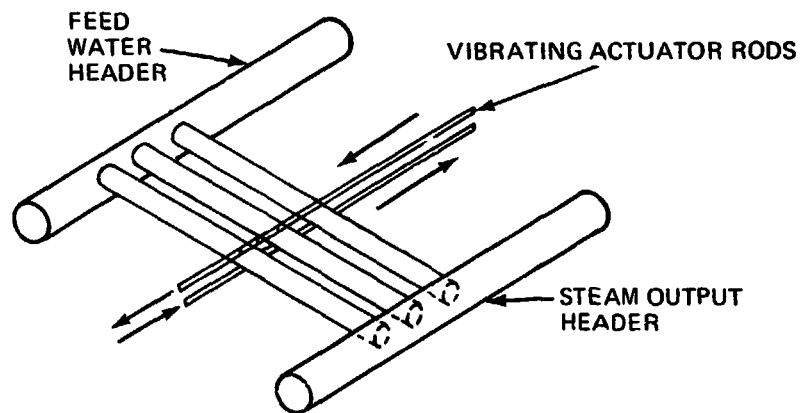
4.2.4 Vibrating Surfaces

Mechanical vibration is used in selected applications to remove loosely agglomerated solid particles from surfaces. If the adhesion forces are small enough, it could be feasible to use this technique to remove the PCM from the heat exchanger surfaces (Figure 4-13).

Because of the relatively thick walls needed for a high-pressure sink fluid, the heat exchanger will be relatively stiff and massive. Bellows would be required to isolate the vibrating mass from the rest of the system, and the bellows would have to contain the high-pressure sink fluid. Adhesion data would be required to permit design of this system. While perhaps feasible, this system seems to present more problems and no advantages over a vibrating liquid system (ultrasonics).

An alternate arrangement which eliminates the bellows is to use an array of parallel thin walled tubes, all connected to relatively stiff headers at both ends. The tubes would have attachment lugs at their midpoints and put in torsion by push rods (somewhat in the fashion of the slat rotation of venetian blinds). This has the advantage of applying a relatively uniform strain over the tube surfaces, which would not be the case with bending vibrations. The natural frequency of the tubes in torsion would be well above the actuator frequency, so there would be no resonance effect.

BELLOWS
ISOLATOR

MECHANICAL OR
ULTRASONIC HORN
TO VIBRATE
TUBING

BELLOWS

GAS BLANKET

FEED
WATER
INPUT

STEAM
OUTPUT

LIQUID PHASE

SOLID PHASE

HIGH
PRESSURE
STEAM
INPUT

OUTPUT

LOW PRESSURE
SALT STORAGE
TANK

2153-025(W)

(a) Shaker Concept

FEED
WATER
HEADER

VIBRATING ACTUATOR RODS

STEAM OUTPUT
HEADER

(b) Torsion Concept

1767-022(T)

Figure 4-13 Proposed Vibrating Heat Exchanger Concepts

4.2.5 Vibrating Liquid (Ultrasonic)

This concept would employ ultrasonic horns located in proximity to the heat exchanger tubes as shown in the single-tank arrangement in Figure 4-14. The tubes would be located just below the lowest liquid level (when the tank contains the maximum solid), and the salt quantity would be such that after the design heat usage, sufficient liquid remains to cover the tubes.
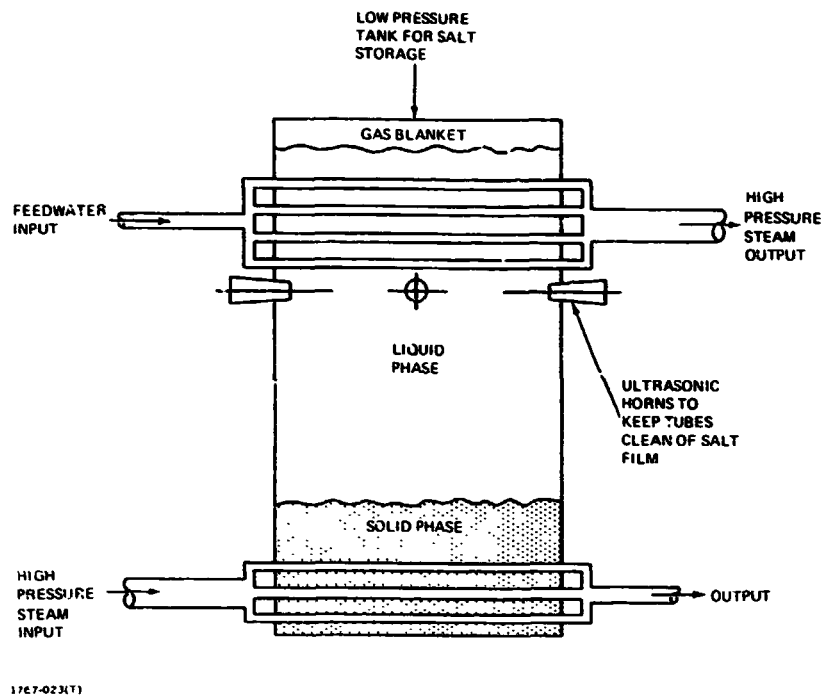
LOW PRESSURE
TANK FOR SALT
STORAGE

GAS BLANKET

FEEDWATER
INPUT

HIGH
PRESSURE
STEAM
OUTPUT

LIQUID
PHASE

ULTRASONIC
HORNS TO
KEEP TUBES
CLEAN OF SALT
FILM

SOLID PHASE

HIGH
PRESSURE
STEAM
INPUT

OUTPUT

17E7-023(T)

Figure 4-14 Proposed Heat Exchanger Utilizing Ultrasonics to Keep Tubes from Getting Salt Buildup

The ultrasonic horns cause cavitation of the liquid which erodes solid salt particles off the tubes analogous to ultrasonic cleaning, which is a standard industrial process. In addition to the horns, the only other equipment needed is the horn power supply and convertor which converts from line voltage (117 VAC 60 Hz) to the ultrasonic frequency used (typically 20 kHz).

No molten salt pumps are shown for the single-tank concept shown in Figure 4-14 and the unit could be of modular construction with each tank loaded with salt, purified, and sealed at the factory. While this single-tank natural convection system appears to be the most simple approach there may be a problem in locating horns with sufficient power and adequate cooling close enough to the heat exchanger surfaces. The power required by the

ultrasonic horns can be appreciable, and may influence the choice between the natural convective and pumped approach. Ultrasonics have been identified as a possible concept for this high-temperature application because similar requirements exist in systems designed for fluxless soldering.

4.2.6   Tube Flexing

Tube flexing is another alternative to scraping the salt off the surface by inducing motion in either the tube or salt as was done in the vibrating and ultrasonic systems. In this concept, however, instead of externally applied energy, the energy is extracted from the heat sink fluid.

As indicated schematically in Figure 4-15, flexing of the heat exchanger tube to shed the salt layer is obtained by cycling the internal pressure by using an in-line oscillator valve. Because of the high pressure of the sink fluid, the tube walls are already thick from a structural point of view and must be thickened further to accommodate the flexure stress. Also, with flexure, some portions of the surface (nodal points) experience little strain and may present a salt buildup problem. Hence, while the concept is basically simple, there are technical questions to be answered in finding suitable shapes with reasonable pressure cycling needed above the normal steam pressure to minimize salt buildup and the effect of this cycle on the fatigue life.
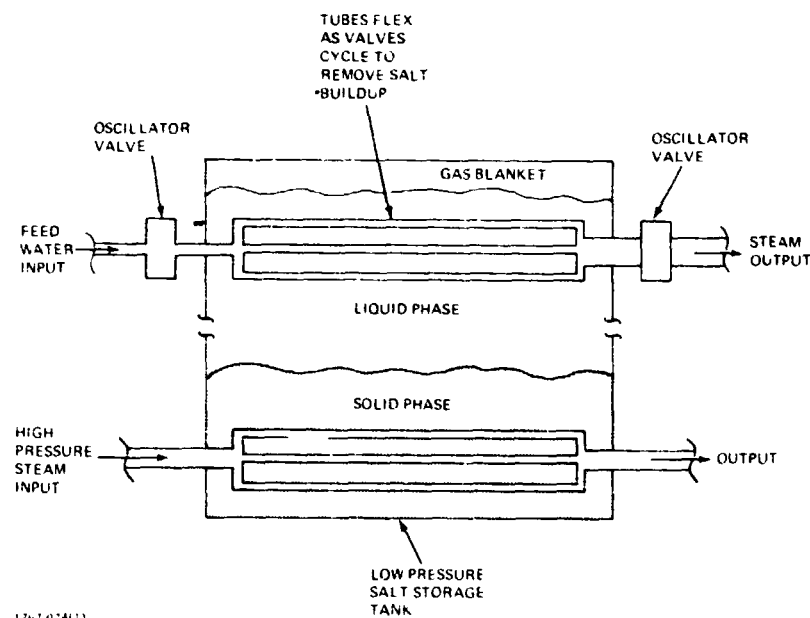

Figure 4-15 Proposed Heat Exchanger Tube Flexing thru Pressure Pulsing by Throttling Valving

4.2.7 Liquid Bath With Gas Bubble Turbulation

The gas bubble turbulator concept shown in Figure 4-16 uses a pulsating stream
of nitrogen bubbles to stir the molten salt and to remove the solidified salt from the tubes.
It is otherwise similar to a passive design except that it requires more salt (because
complete solidification is not possible) and fewer tubes. The success of this design requires
very low adhesion strength between the salt and tube surface, which could be obtained by
using suitable nonstick coatings. Laboratory scale test verification would be needed before
further serious consideration is given.
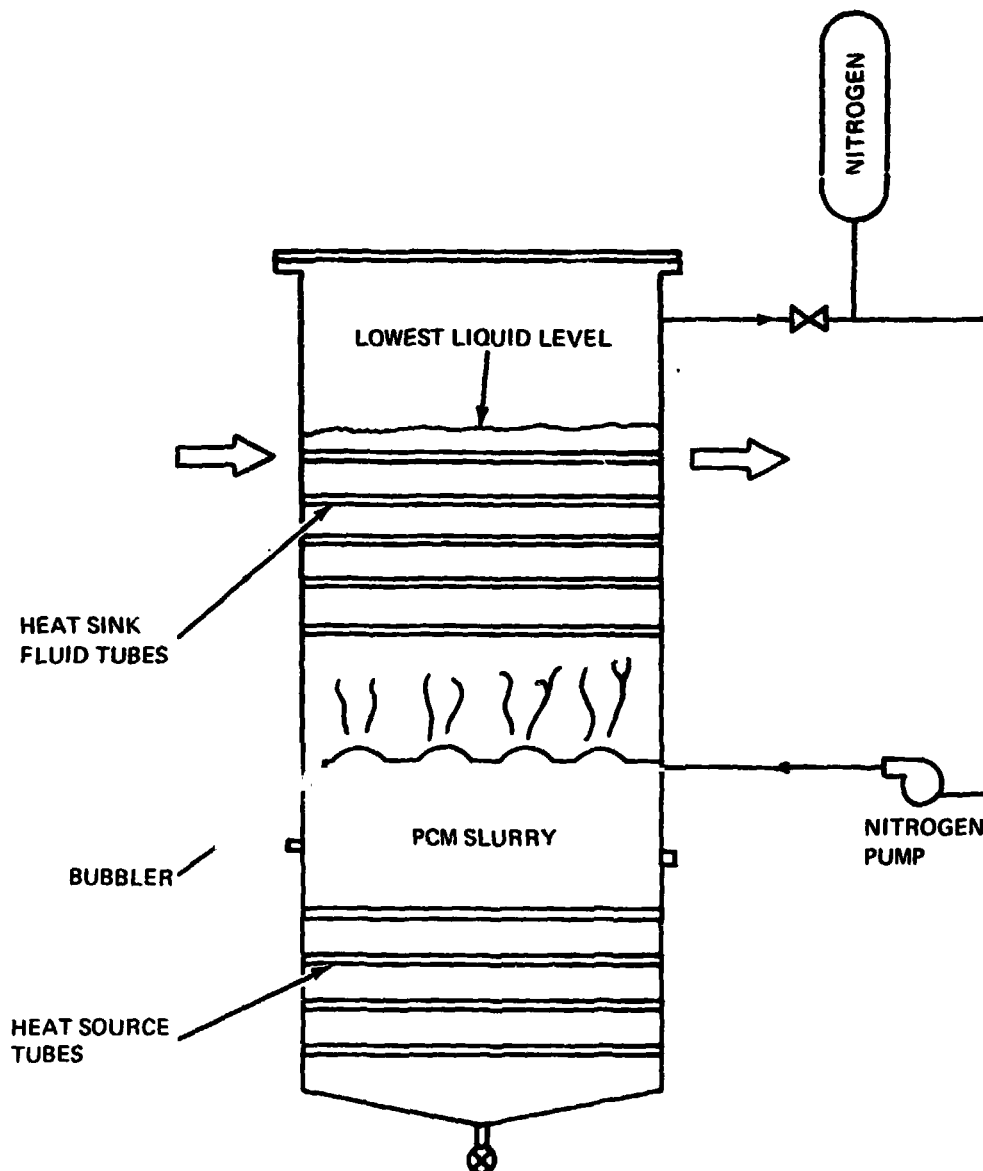
1767-025(T)

Figure 4-16 Gas Bubble Turbulator HX Concept

4-24

4.2.8 Spray Freezing (Direct Contact Heat Exchanger)

This approach is fundamentally different from the others discussed in that there is no heat exchanger area required to remove heat from the salt. Molten salt is sprayed into a lower melting point carrier fluid. The carrier fluid is initially at a temperature below the salt freezing point. The salt droplets transfer heat to the carrier fluid, increasing its temperature, and freeze into solid particles which are contained in the carrier fluid. The particles could then be separated out in a storage volume containing the heat storage heat exchanger as in the other concepts. The overall system schematic was discussed in paragraph 4.1.5 and shown in Figure 4-5.

Although this approach eliminates the salt heat exchanger for the heat usage portion of the utility cycle, a carrier fluid to utility fluid heat exchanger is still required. Because high heat transfer coefficients can be obtained for flowing liquids, particularly if the carrier is a liquid metal, this heat exchanger will be very efficient. Also, it may be desirable from a safety point of view to use an intermediate liquid metal loop to minimize chemical reactions with the PCM in the event of leakage, independent of the type of active heat exchanger used. In this case, a spray freezing process would be one of the simplest and cheapest systems to implement.

4.2.9 Nonstick Coatings

Several of the concepts previously discussed, the mechanical vibrator, the ultrasonic liquid bath, flexible tubes with pressure pulsations, gas bubble turbulator, depend in different ways on the inertia of the thin solid layer of PCM in overcoming the adhesive forces between the solid PCM and the heat exchanger surface. If the adhesive force could be reduced, either the solid layer thickness or the induced motion could also be reduced, with corresponding performance improvements and/or power input savings. The use of thin nonstick coatings (such as Teflon or polished nickel plate) on the heat exchanger should be considered for this purpose. Also, if nonstick coatings can be found which are particularly effective, it may be possible to design heat exchanger surfaces which naturally shed the solid layer with no active motion required (e.g., downward facing horizontal surfaces).

4.2.10 Conductivity Enhancing Additives

The basic objective of active heat exchangers is to remove the solid salt layer from the heat exchanger surfaces to minimize solidified salt thermal resistance. With

some of the systems (translating scraper, and rotating drum), however, the solid layer thermal resistance remains significant (or dominant), and, in these cases, the use of conductivity enhancers could significantly improve performance.

The enhancers would be compatible metals in the form of powders or chopped fibers, fine enough to remain dispersed relatively uniformly in the PCM. They should not affect the active elements of the heat exchanger through either erosion or corrosion. However, it will be necessary to show that enhancers are cost effective in a net sense (direct material cost plus increased system costs for larger tanks, pumps, power, etc., minus savings in the active heat exchanger size and power).

5.0 EVALUATION OF CANDIDATE ACTIVE HEAT EXCHANGER CONCEPTS

5.1 REFFRENCE TES APPLICATION

The reference application selected as the basis of comparison is a 100 MW_e solar central receiver power plant which would require approximately 300 MW_t. Heat is to be stored at a temperature which can produce boiling at 350°C, 16.5 MPa (662°F, 2400 psi). The maximum storage time is 6 hr, so that a total storage of 6 x 300 = 1800 MWh_t is required (6.14 x 10^9 Btu). A liquid metal or salt is assumed for the interface fluid so that all tubes and piping may be designed for low pressures. Further, for ease of construction and transport, the maximum size of any individual component is limited to what can be transported on a standard railway flat car, 12 ft (3.7 m) dia. and 40 ft (12.2 m) long. The storage media is the selected chloride salt eutectic (KCl•NaCl•MgCl$_2$).

5.2 PASSIVE DESIGN

To serve as a standard for cost and performance comparisons, a passive TES system was formulated consisting of shell and tube heat exchangers (see Figure 5-1).
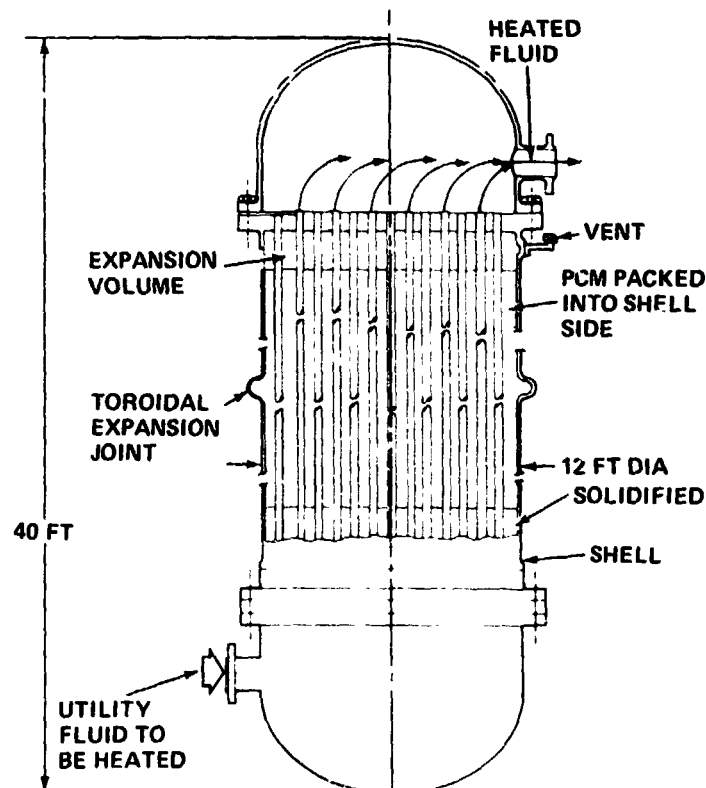
1767-026(T)

Figure 5-1 Passive TES Shell and Tube Heat Exchanger Concept

Assuming one dimensional heat transfer and neglecting the sensible heat storage of the salt, the following expression can be used to describe the relationship between the solidification radius, R, and time, t.   (5.1)

$$\left(\frac{R}{r_o}\right)^2 \ell n \left(\frac{R}{r_o}\right)^2 + \left[\left(\frac{R}{r_o}\right)^2 - 1\right] \left\{ \frac{2k_s}{r_i} \left[\frac{1}{h} + \frac{r_i}{k_w} \ell n \left(\frac{r_o}{r_i}\right)\right] - 1 \right\} = \frac{\left(T_f - T_m\right) 4 \, t k_s}{\lambda \, \rho_s r_o^2}$$

The solidification radius, R, is equal to one-half the tube spacing and

h = fluid film coefficient

r_i = pipe inner radius

r_o = pipe outer radius

k_w = pipe wall thermal conductivity

k_s = solid state salt thermal conductivity

T_w = pipe outside wall temperature

T_m = salt melting point

T_f = fluid bulk temperature

λ = salt latent heat of fusion

When the internal heat transfer conductance within each tube is very large, Equation (5.1) can be simplified to give:

$$\left(\frac{R}{r_o}\right)^2 \ell n \left(\frac{R}{r_o}\right)^2 + \left[1 - \left(\frac{R}{r_o}\right)^2\right] = \frac{\left(T_f - T_m\right) 4 \, t k_s}{\lambda \, \rho_s r_o^2} \qquad (5.2)$$

Assuming 1-in. diameter tubes (r_o = 0.5 in. = 1.27 cm) and a ΔT = 28°C (50°F), Equation (5.2) yields a required tube spacing of 10.27 cm (4.2 in.) for a 6-hr discharge cycle.

For a given mass of salt, m_s, the required number of tubes, N, of length, L, is given by

$$N = \frac{m_s}{L \, \rho_1 \, \pi \, (R^2 - r_o^2)} \qquad (5.3)$$

where ρ_1 = salt liquid density.

Assuming that the tubes are on hexagonal centers, a TES module diameter can be estimated from the total cross sectional area per tube as follows:

$$D_m = 2 \sqrt{N (2R)^2 \left(\frac{\sin 60}{\pi}\right)} \qquad (5.4)$$

For the reference application the required salt mass is $Q/\lambda = 22.1 \times 10^6$ kg (48.7 $\times 10^6$ lb). Using a limiting module diameter of 3.7 m (12 ft), each cylinder can contain 1200 tubes, hexagonally spaced. For a length limit of 12.2 m (40 ft) and allowing space for expansion upon melting and a nitrogen blanket atmosphere, about 130 tanks will be needed.

The cost of a tank module can be estimated from the total weight of material Using stainless steel materials and a shell wall thickness of 1.27 cm (0.5 in.) and a tube thickness of 0.0673 cm (0.025 in.), the following summarizes the material volume and cost for one module.

	Material Volume (ft^3)	Cost
Tank:	82. @ $1.10/lb	$ 43,850
Tubes:	55. @ $2.10/lb	$ 56,340
Total material cost:		$100,190
Labor (welding & assembly) cost:		$150,000
Total cost per module:		$250,190

For 130 units the total cost for the heat exchanger modules will be $32,524,700, without salt. Assuming 10¢/lb for the salt, the total cost for the passive TES system will be $37,398,000, which is about 21 $/kWh$_t$ on a unit basis.

This design assumes use of latent heat only, proper consideration of sensible heat would reduce the number of heat exchangers from 130 to as few as 95, with a corresponding reduction in cost.

The technical weaknesses of this passive design are mainly in its ability to provide constant power. As the solid salt layer grows, the heat transfer resistance goes up dramatically and the rate of heat flow decreases.

5.3   ACTIVE DESIGNS

The concepts which involve mechanical distortion or abrasion of the heat transfer surfaces (vibrators, ultrasonics, tube flexing) were eliminated after the initial preliminary evaluation because the associated development risks were judged much greater than those of other candidate systems. The remaining candidates were therefore confined to the scraper concepts, gas bubble turbulation with nonstick surfaces, and direct contact heat exchange.

5.3.1   Scraper Designs

An adequate performance evaluation of the candidate scraper concepts can be obtained by grouping them into one generic family.

The active scraper heat exchanger provides increased heat flux compared with a passive salt bath heat exchanger by incorporating some technique for removal of salt depositions from the heat transfer surfaces, thereby eliminating the thermal resistance of the solidified layer. To provide an indication of the magnitude of this effect, a one-dimensional analysis is used for the propagation of a solid liquid interface away from a uniform temperature wall, cooled on the backside by the sink fluid. Assuming a linear temperature variation through the wall and through the solid PCM, the solid layer thickness is given by:

$$X = \frac{k_s}{U} \left(\sqrt{1 + 2q_o t/B_o} - 1 \right)$$

and the mean heat flux over the time interval, t, by

$$(q/A) = (B_o/t) \left(\sqrt{1 + 2q_o t/B_o} - 1 \right)$$

where $U = \left[1/h + t_w/k_w \right]^{-1}$

$$q_o = U (T_m - T_o)$$

$$B_o = \lambda \rho_s k_s/U$$

with h = film coefficient

t_w = wall thickness

k_w = wall conductivity

k_s = solid PCM conductivity

λ = heat of fusion

ρ_s = PCM solid density

Note that q_o is the heat flux with no solid salt thermal resistance.

Using the chosen chloride salt as the PCM (T_m = 725°F (385°C), k_s = .9 Btu/ft hr°F (1.56 W/mK), and ρ_s = 140 lbm/ft^3 (224 kg/m^3)), a stainless steel wall (with t_w = 0.05 in. (0.127 cm) and k_w = 10 Btu/ft hr°F (17.3 W/mK)), and backside fluid flow with T_o = 700°F (371°C) and a film coefficient h = 2000 Btu/ft^{2}hr°F (6300 W/m^2) (corresponding to liquid metal flow) resulting values of (q/A) are shown in Figure 5-2 for time intervals
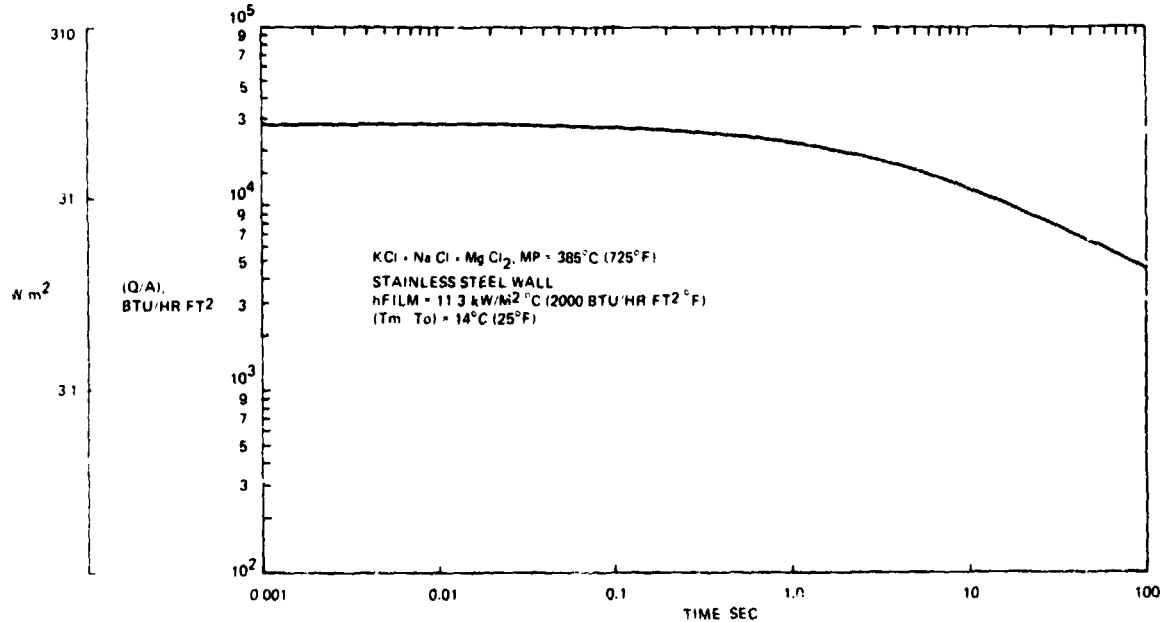

Figure 5-2 Mean One-Dimensional Heat Flux vs Salt Solidification Time

1767-027(T)

ranging from 10^{-3} to 10^2 sec. The zero salt thickness heat transfer rate is 27 x 10^3 $\frac{Btu}{hr\,ft}$2 (85.1 kW/m^2) for this case. There is little fall-off for times of 0.1 sec or less, but a relatively rapid drop for longer times, as salt thermal resistance becomes significant. In considering scraper designs for this example, a scraper would need to scrape a surface 10 times a second to provide near maximum performance. To provide the required design heat flux, the scraping rate and total scraped surface area must be matched. The total required flux is 300 MW$_t$ (1.02 x 10^9 Btu/hr), thus:

Scraping frequency (Times/sec)	Total surface area, ft^2(m^2)
100	37,500 (3486)
10	38,346 (3564)
1	45,414 (4221)
0.1	81,875 (7610)
0.01	210,440 (19,560)

5-5

These values represent a significant reduction in the required total area compared with the passive design value of 898,000 ft^2 (83,470 m^2).

The rotating drum system's effectiveness depends on the thickness of the salt layer on the drum which is related to drum size and speed. Since the drum is not immersed in the molten salt, scraping proceeds unimpeded and the heat transfer is easily controlled.

The tube scraper designs are not so straightforward. Since the scrapers are immersed in the salt, solidification resumes immediately after scraping has occurred. Very fast scraping rates would be required to achieve highest heat transfer rates, since even a thin layer of solid salt can degrade heat transfer significantly.

The basic containment and PCM costs are assummed to be the same as in the passive design. Thus, the cost comparison is between the tubes in the passive design and the scraper mechanism. The most promising scraper design is felt to be the rotating drum scraper since it provides for separation of solid and liquid phases of the salt. It does not require a complicated individual scraper mechanism on each pipe, and it provides for controlled heat transfer rates. A reduction of heat transfer area compared to the passive design of 50 to 70% or even more in a well designed system is possible. On the minus side motors to rotate the drums and rotating unions will be required.

Assuming a cost reduction of 50% with respect to the tube costs of a passive system, i.e., a scraper mechanism cost of about $25,000 per heat exchanger module, the cost of an equivalent scraper module is estimated to be about $222,000. Therefore, the unit cost for the entire TES system will be about 16 $/kWh$_t$.

5.3.2   Gas Bubble Turbulator

The success of the gas bubble turbulator concept relies on the effectiveness of the bath turbulence in removing the salt as it solidifies on the tube surfaces. In theory it is similar to the tube-shell passive design except that it requires more salt (since complete solidification is not possible) and fewer tubes (owing to the improved heat exchange). Since the tubes represent about 25% of the total cost of the passive design, a significant decrease in number would reduce costs. If only half the tubes were needed then the unit TES system cost would be about 15 $/kWh$_t$, depending upon the costs of the nonstick coatings and the nitrogen turbulator loop.

Since this concept relies on a mechanism that was easily verified, laboratory scale element tests were run in support of the evaluation. The objective was a qualitative assessment of the ability to remove solidified PCM from the surface of a tube treated with a nonstick coating. Two types of tests were conducted: 1) a coupon adhesion test with sample materials and the actual chloride salt eutectic, and 2) a visual demonstration using an impinging stream of nitrogen bubbles to break apart solidification of PCM around a cooling tube.

The set-up used for the coupon adhesion tests is shown in Figure 5-3. It consisted of a steel drum with a removable top lid containing an electrically heated resevoir which held the chloride salt eutectic. The lid was equipped with a glass viewing port, a fitting which could be used for either creating a vacuum or pressurizing with nitrogen gas, and an access port for the material test sample. The material coupons evaluated included polished
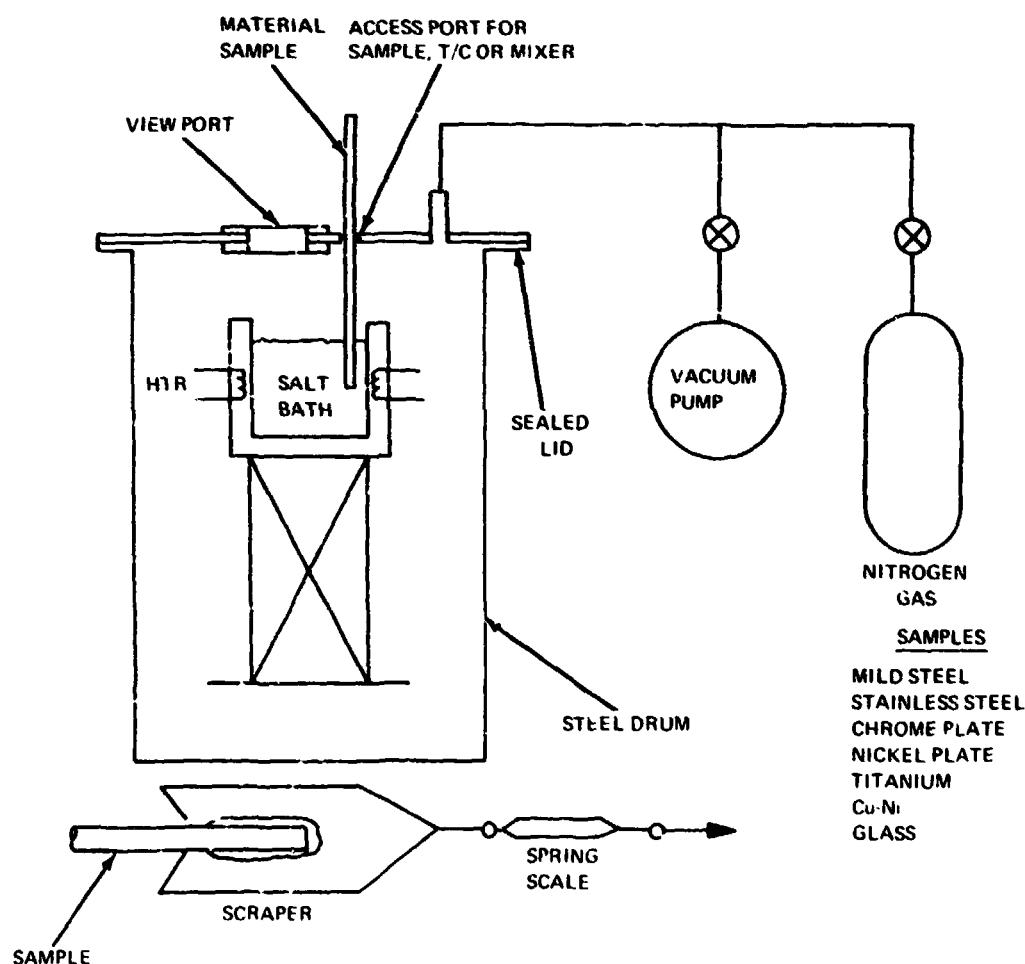

Figure 5-3 Element Test - Salt Adhesion

1767-028(1)

5-7

mild steel, stainless steel, nickel plated steel, chrome plated steel, titanium, copper-nickel and glass. The test procedure consisted of keeping the bath at 425°C, immersing the sample for 25 seconds, withdrawing it and immediately scraping the surface. Although qualitative, the results clearly indicated that the polished chrome plated and nickel plated samples had the least salt buildup and lowest surface adhesion strength. These results agreed with the opinion of molten salt consultant, Dr. George Janz, who suggested using polished nickel plate based on camparable data published for flouride salts which he thought should be similar in behavior to the chlorides.

The test setup used to evaluate bubble turbulation is shown in Figure 5-4. A pyrex container was used to hold the test bath and a controllable temperature glycol loop provided the cooling for the sample tubes, which were either polished stainless steel or teflon. The
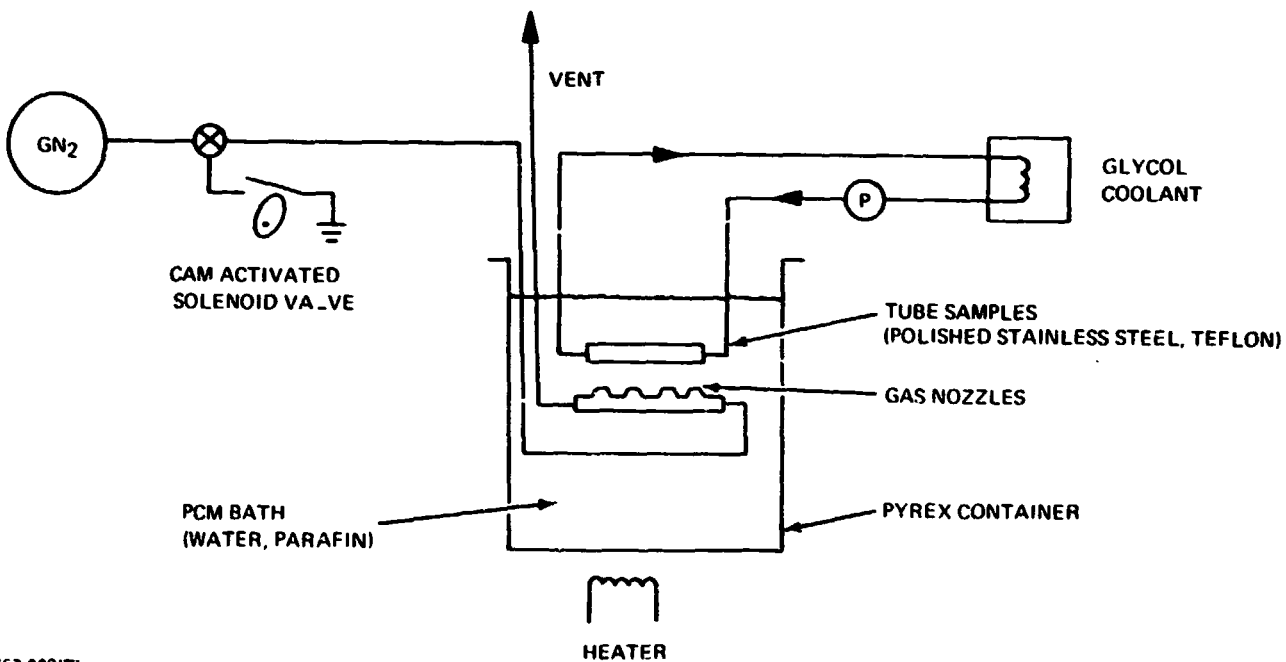
1767-029(T)

Figure 5-4 Element Test - Gas Bubble Turbulator

teflon was used since its nonstick qualities are well known. If the concept did not work with the teflon tube, it would not work with anything. Initial tests using a water-ice bath showed that the gas bubbles had no disruptive effect on the formation of solid ice around the tube, regardless of the material. The only difference with teflon was that the ring of ice took longer to form. Since water is not a typical fluid, additional tests were run using paraffin (melt point ~ 108°C) as the phase change material. Test results were the same; a ring of PCM formed around the tube for all test conditions.

The negative results for these two element tests were enough to discourage further development of the bubble turbulator concept. Namely, the chloride salt sticks to all tube surfaces and the surface turbulence caused by impinging gas bubbles is ineffective in removing a PCM from even the most nonsticking of surfaces – teflon.

5.3.3 Direct Contact Heat Exchanger

The amount of salt and the heat exchanger shell design are the same as in the passive system, but this design substitutes the liquid metal carrier fluid loop for the closely spaced tubes of the passive design. Therefore to be competitive, the cost of the liquid metal, salt and liquid metal pumps, and flow systems must be less than the cost of the tubes in the passive case. For this evaluation a 44.5 Pb/55.5 Bi eutectic was used for the liquid metal carrier fluid since it is compatible with the chloride salt eutectic.

The direct contact heat exchange design analyzed includes three tank modules that are coupled by two separate fluid loops; one for a molten salt, and another for a liquid metal carrier. The salt serves as the thermal energy storage medium while the liquid metal transfers the stored energy to the utility heat sink. Two modules contain separate quantities of liquid metal and molten salt. These are then brought together in the third module which is the actual heat exchanger. Both latent and sensible heat are transferred to the cooler liquid metal by a countercurrent flow of molten salt bubbles.

The principal concerns of the direct contact heat exchanger design for the reference application are the size and depth of the liquid metal tank and the salt and metal pump sizes. The necessary heat transfer for each of the 130 modules is 2.3 MW$_t$ (7.86 E06 Btu/hr) which requires a salt flow rate of 80 gpm and a liquid metal flow rate of 900 gpm, assuming a 27°C temperature rise in the liquid metal. The salt injector is sized to create drops of molten salt about 1/8 in. (3.2 mm) in diameter which will rise through the metal at about 1 ft/sec (0.3 m/sec) and solidify after travelling about 1 ft (0.3 m).

The terminal velocity of a rising salt bubble $(\overline{V}_t)$ can be obtained by equating the buoyancy force to the drag and then solving for velocity.

$$\overline{V}_t = \left[\frac{4}{3} \frac{(\rho_f - \rho_L)}{\rho_f} \frac{d}{C_D} \right]^{1/2}$$

where

ρ = density (f = carrier fluid, L = liquid salt)
d = bubble diameter
C_D = drag coefficient for a sphere

5-9

The residence time required to solidify a molten salt bubble which is rising through a counterflowing stream of liquid metal can be calculated by quantifying the heat transfer to the fluid associated with each solidifying bubble. The results are summarized as follows.

$$
t = \frac{a\, \rho_s\, C_{Pf}}{3B} \left\{ \frac{a}{k_s \varphi} \left[\frac{1}{2} \ln \frac{\left(\dfrac{\varphi^2 - \varphi + 1}{(\varphi + 1)^2} \right)}{\left(\dfrac{\varphi^2 - \alpha\varphi + \alpha^2}{(\varphi + \alpha)^2} \right)} + \sqrt{3} \left[\tan^{-1}\left(\frac{2 - \varphi}{\sqrt{3}\,\varphi} \right) - \tan^{-1}\left(\frac{2\alpha - \varphi}{\sqrt{3}\,\varphi} \right) \right] \right] + \left(\frac{1}{h} - \frac{a}{k_s} \right) \ln \frac{A+B}{(A+B\alpha^3)} \right\}
$$

where

$$
A = \frac{C_{Pf}(T_m - T_{fo})}{\lambda} + \left(\frac{\dot{m}_s}{\dot{m}_f} \right) \left(\frac{\rho_s}{\rho_L} \right)
$$

$$
B = -\left(\frac{\dot{m}_s}{\dot{m}_f} \right) \left(\frac{\rho_s}{\rho_L} \right)
$$

$$
\gamma = \left(\frac{A}{B} \right)^{1/3} = (-1) \left[\left(\frac{\rho_L}{\rho_s} \right) \frac{\dot{m}_f C_{Pf}(T_m - T_{fo})}{\dot{m}_s \lambda} + 1 \right]^{1/3}
$$

$$
\alpha = \left(1 - \frac{\rho_L}{\rho_s} \right)^{1/3}
$$

and

a   = bubble outside radius

C_{pf} = specific heat of carrier fluid

h   = outside film heat transfer coefficient

ks = thermal conductivity of solid salt

$\dot{m}_f$ = mass flow rate of carrier fluid

$\dot{m}_s$ = mass flow rate of salt

Tm = salt melt temperature

T_{fo} = carrier fluid outlet temperature (hot)

ρ = salt density (s = solid, L = liquid)

λ = salt latent heat of fusion

The foregoing equation solves for the required residence time. However, the actual residence time available with a given design is determined by the net upward bubble velocity and the length of fluid column. The net bubble velocity is the difference between the terminal velocity of the bubble and the countercurrent carrier fluid velocity.

$$\overline{V}_b = \overline{V}_t - \overline{V}_f$$

therefore

$$t_{actual} = \frac{L_{column}}{(\overline{V}_t - \overline{V}_f)}$$

Theoretically $\overline{V}_f$ must always be less than or equal to $\overline{V}_t$, or else the bubble would stagrate. However, the recommended values of $\overline{V}_f$ which are derived from empirical design data limit the velocity to about 10% of the dispersed stream (salt) velocity, so $\overline{V}_f < \overline{V}_t$. This restriction prevents flooding of the tower, wherein there is a high hold-up of the dispersed phase in the column with the mass of salt bubbles extending down to the base. The length of the required column can be calculated once the residence time and flow velocities are known.

The complete system design requires about 0.6×10^6 kg (1.3×10^6 lb) of metal eutectic, 130 metal pumps (one for each shell) capable of 900 gpm against 345 kPa (50 psi) and 130 molten salt pumps each capable of 80 gpm against 207 kPa (30 psi). The total liquid metal cost will be only 2.60×10^6 so that about \$17. $\times 10^6$ will be left for pumps and flow system to match the cost of the passive system. This allows roughly \$130,000 per shell for both pumps. Since the cost of a currently available submersible pump for conventional liquid metal pumping at 600 gpm is \$17,000 for the pump and motor, a cost effective pump can be developed for this application.

Unlike the passive system, this design will be able to provide the desired full rated power output at any time. It will be more efficient thermodynamically due to the high rates of heat transfer attainable. Power requirements for the pumps are estimated to be small, about 1.8 kW for the metal and 0.7 kW for the salt.

The costs for one module are estimated as follows:

Salt/metal tank:	$ 50,000
Pumps (2):	$ 34,000
Plumbing & controls:	$ 10,000
Labor:	$ 75,000
Salt:	$ 37,460
Liquid metal:	$ 20,000
Total module Cost:	$226,460

The total system cost will be about $29.4E06 or about $16\$/kWh_t$ on a unit basis.

There could be variations and uncertainty associated with the foregoing cost estimates for the various TES systems depending upon the actual system development costs and the production quantity. The cost estimates given herein should be treated as a relative comparison between systems rather than as absolute values.

5.4   RECOMMENDATION

The two active heat exchanger concepts recommended for demonstration hardware development are the direct contact heat exchanger and the rotating drum scraper. The former is the most cost competitive approach and also uses readily available technology, which minimizes development risk. Of all the scraper concepts considered, the rotating drum was selected because it promised the most benefits over the tube intensive passive design. In addition, versions of the translating scraper and internal drum scraper have been previously built by Honeywell and G. E., respectively.

6.0 DESCRIPTION OF ACTIVE HEAT EXCHANGER CONCEPTS FOR DEMONSTRATION HARDWARE DEVELOPMENT

6.1   SYSTEM

The active TES heat exchanger system for the test evaluation is shown schematically in Figure 6-1; only the major elements are illustrated. It consists of three basic com-
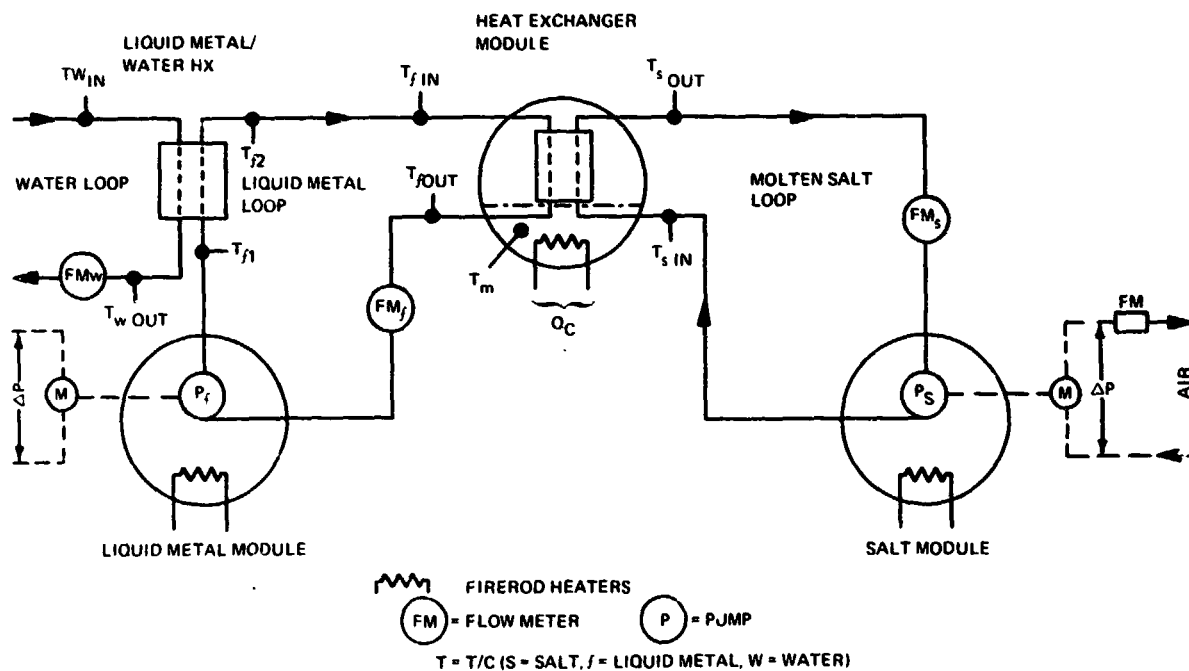
Figure 6-1 Demonstration Active TES System Schematic

ponents: the central heat exchanger module; a salt module; and a liquid metal module. In all cases the storage medium is a chloride salt eutectic (20.5 KCL • 24.5 NaCL • 55.0 $MgCl_2$) and the heat transfer fluid is a liquid metal lead-bismuth eutectic (44.5 Pb • 55.5Bi). The nominal melting points are 385°C (725°F) for the salt and 125°C (257°F) for the metal.

The central heat exchanger module can be readily configured to contain either of the heat exchanger concepts. This is done by simply replacing the top half of the tank with the necessary hardware. The bottom half, which serves as the storage bin for the solidified salt, is used by both concepts. It also contains electrical firerod heaters which are used to melt the salt during the thermal charging cycle. These heaters simulate the fluid heat source of an actual application. As the salt melts, it drains into the salt module. This

6-1

module acts as a holding tank for the molten salt. It also contains a submersible pump, driven by an air motor, which is used to pump the molten salt to the heat exchanger module during the discharge part of the demo cycle. Firerod heaters are provided to control the initial salt temperature and to prevent inadvertent solidification.

The liquid metal is used as a heat transfer fluid to remove the heat from the molten salt, which takes place within the heat exchange module. The metal is stored in the liquid metal module which also contains the pump used to pump it through the heat exchanger. Electrical heaters are provided to control the liquid metal temperature.

During the thermal discharge cycle operation, the heat picked up by the liquid metal from the molten salt is transferred to an open water cooling loop through an annular heat exchanger. The cooled metal is then returned to the heat exchange module where it can once again serve as an acceptable heat sink. This process continues until all of the molten salt has been solidified, then the charging cycle can be started again.

All of the tanks and plumbing are insulated with high temperature JM Cerablanket insulation, with thermal losses estimated at less than 5 percent. Thermocouples are provided both within the tanks and on the outside surfaces of the plumbing.

6.2   DIRECT CONTACT HEAT EXCHANGER

The concept for the direct contact heat exchanger demonstration test module is shown in Figure 6-2. Solid chloride salt is held in the bottom of the central heat exchanger module (tank H). During the charging cycle, thermal energy is stored in the salt by using electrical heaters which simulate the fluid heat source of an actual installation. The salt melts, aided by natural convection, and drains into a separate molten salt holding tank (module S). During the usage cycle, heat is removed from the salt by direct contact heat transfer with a liquid metal carrier fluid within the heat exchange reservoir. Both the heat storage and carrier fluids must be completely nonreactive and immiscible with each other. The molten salt is pumped from the holding tank into the bottom of the heat exchange reservoir where because of its lower density, it bubbles through the metal giving up its heat as it solidifies. At the same time, the heated liquid metal returns to its holding tank (Module M) from where it is pumped to a conventional external heat exchanger. Here the liquid metal releases its energy to the ultimate heat sink fluid (water in the case of this demo unit). The cooled liquid metal is then returned to the top of the heat exchange

reservoir where it can once again be heated. As the solid salt agglomeration rises to the top of the heat exchange reservoir, it is directed over the edges and falls to the bottom of the surrounding tank. It remains there until the next charging cycle, when the entire sequence is repeated.
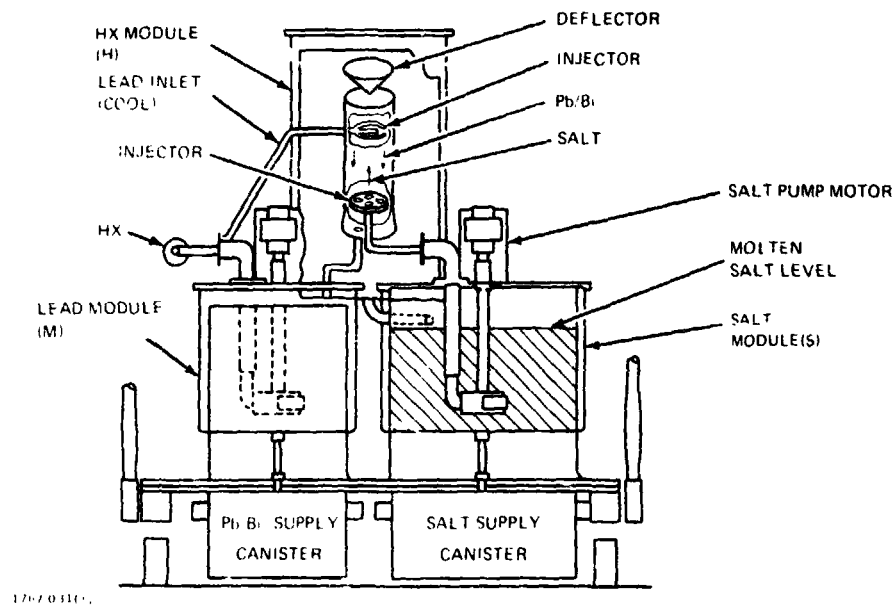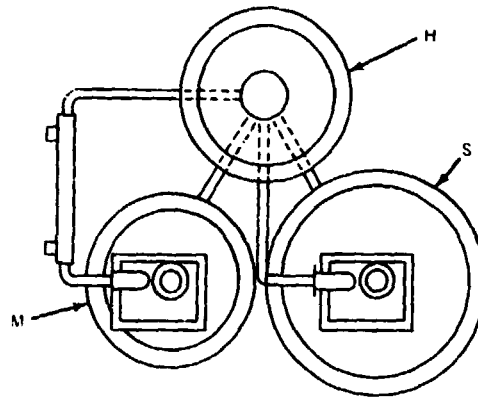

Figure 6-2 Direct Contact HX Concept

The total quantity of salt is determined by the energy storage requirement and increases accordingly. However, the amount of liquid metal is separate from energy storage considerations and is mainly determined by the height of the reservoir required to insure solidification of the salt, and the tare volumes of associated plumbing and pumps. It would not be significantly impacted by the increased thermal energy storage capacity

needed for larger systems since only the mass flow rate is important, which only means larger pumps and plumbing. As with all of the molten salt heat exchanger concepts, a dry nitrogen gas blanket is provided to minimize atmospheric contamination.

The overall design of the active heat exchanger concept is summarized below.

System Requirements

- Energy storage   = 10 kW_t hr

- Heat transfer   = 10 kW_t

Selected Media

- TES: 20.5KC1 • 24.5 NaC1 • 55.0 $MgCl_2$ eutectic (mp = 385-396°C, 725-745°F)

    Quantity = 182 kg (400 lb)
    Flow rate = 2.5 kg/min (5.5 lb/min)

- Carrier Fluid: 44.5Pb/55.5 Bi eutectic (mp = 125°C, 257°F)

    Quantity = 409 kg (900 lb)
   Flow rate = 184 kg/min (406 lb/min)

Component Sizing

	Net Volume, M^3 (in.^{3})
Molten salt module:	0.14 (8755)
Liquid metal module:	0.04 (2399)
HX module:	
- HX canister:	0.02 (1372)
- Solid salt space:	0.12 (7268)

All tanks and piping are made from 1020 mild steel or equivalent, except for the two charge/drain canisters and the liquid metal/water heat exchanger which are made from stainless steel. A gaseous blanket of dry nitrogen at 34.5 kPa (5 psig) is used to protect the system from moisture and corrosion.

6.3   ROTATING DRUM SCRAPER

The rotating drum heat exchanger concept minimizes the required heat transfer surface area by eliminating most of the thermal resistance within the solidified storage

medium (e. g. , salt). This is accomplished by the action of a fixed scraper blade which continually removes the solid salt buildup and keeps the liquid solid interface close to the heat exchange surface. The concept as proposed for this demonstration test module is illustrated in Figure 6-3.
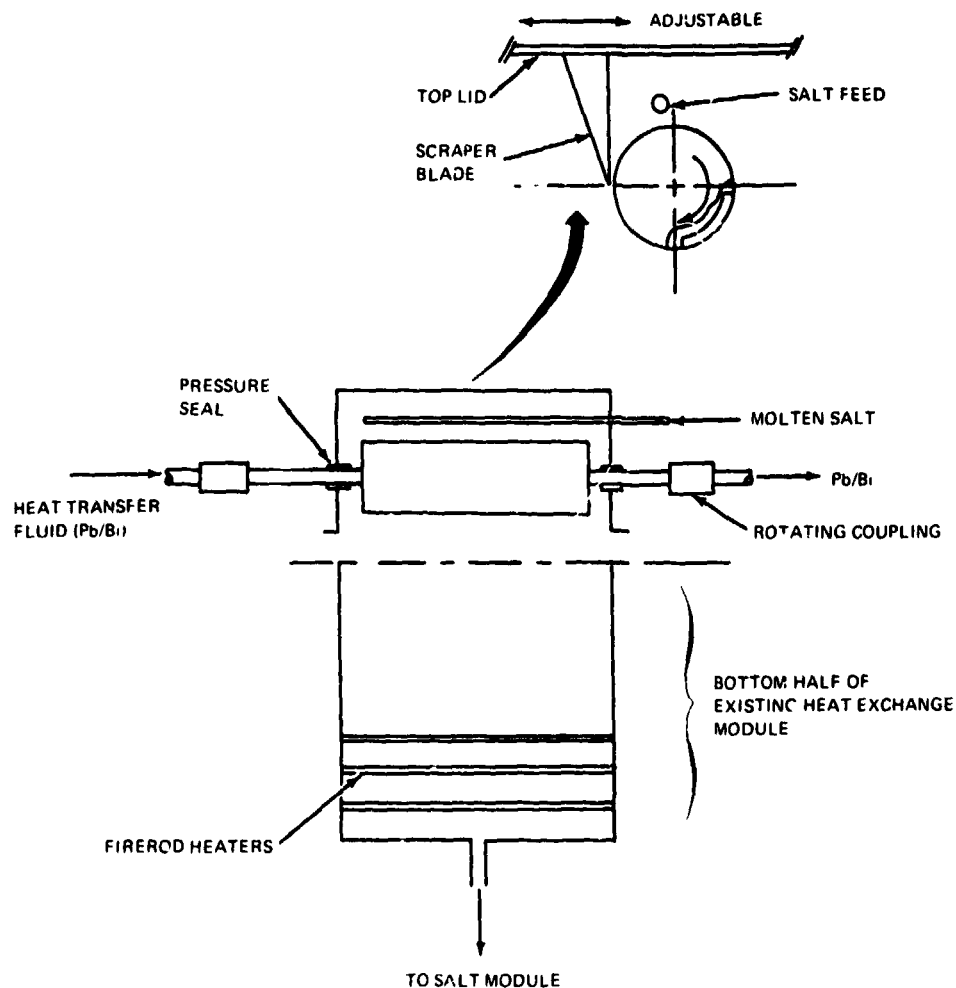
1767-002(1)

Figure 6-3 Rotating Drum Heat Exchanger Concept

During the usage or discharge cycle (heat removal from storage), the molten salt flows through slit nozzles onto the circumference of the rotating drum. The liquid metal heat sink fluid flows through an annular passage within the drum, cooling the outer surface and freezing the molten salt. The solidified layer of salt is then scraped off after making a partial (270 degree) rotation, falling into a storage bin which is located beneath the drum. The storage bin also contains a source fluid heat exchanger which is used to melt the salt during the charging cycle. As an example, the heat source fluid for an actual application could be the collector fluid from a solar central receiver. However, as a simplification,

this demonstration unit uses electrical firerod heaters to simulate the heat source. The melted salt drains by gravity into the molten salt canister where it is stored until needed for the discharge part of the cycle.

The mechanical design of the rotating drum is complicated by the need for rotating fluid couplings at the inlet and outlet connections. The support bearings employ pressurized gas seals with the same inert gas (nitrogen) as that used to provide the protective gas blanket over the salt. Thus, any leakage will be outward to preclude salt contamination. The rotating fluid couplings are standard commercially available hardware.

The system and component specifications are identical to the direct contact heat exchanger concept except for the top half of the central heat exchanger module. The design details peculiar to the rotating drum are given below.

Drum module:	Diameter = 0.61 m (2 ft)
	Height = 0.31 m (12 in.)
Rotating drum:	Outside Diameter = 152 mm (6 in.)
	Internal Flow Annulus = 6.35 mm (0.25 in.)
	Active Length = 432 mm (17 in.)
	Speed = 60 rpm

6.4   PERFORMANCE REQUIREMENTS

Each of the demonstration active heat exchanger concepts has been designed for the following overall thermal requirements:

- Energy storage capacity = 10 kWh$_t$

- Heat transfer rate = 10 kW$_t$

Thus the demo systems should provide complete thermal discharge within one hour.

The anticipated system application calls for generating steam at 350°C (662°F), which would set the desired liquid metal inlet temperature to the heat exchanger module at about 356°C (672°F) (allowing for a 5.5°C pinch point). The melting point of the molten salt is 365°C. By selecting a 22°C (40°F) temperature rise for the heat transfer fluid, which corresponds to a heat exchanger effectiveness of 80%, the flow rates for this nominal design condition are 84 kg/min (400 lb/min) for the liquid metal and 2.5 kg/min (5.5 lb/min) for the molten salt.

The general test objective is to demonstrate a 10 kWh$_t$ storage capacity and a 10 kW$_t$ heat recovery rate at the nominal design conditions. However, there will be specific performance criteria that will be measured in order to permit a realistic assessment of each concept and determine the viability of larger scale demonstration units.

Multiple charge/discharge cycles will be run to evaluate the following:

- Percentage energy recovery
- Energy expended for heat recovery
- Efficiency of energy recovery (energy recovered-energy expended)/energy recovered
- Heat transfer rate as a function of time
- Effect of varying critical parameters (flow rates, inlet temperatures, drum speed, etc.)
- Heat losses from system

7.0 REFERENCES

1. Ferrara, A., Haslett, R., and Yenetchi, G. "Final Report, Latent Heat Thermal Energy Storage Heat Exchanger," NASA CR 135244

2. Boser, O., "Study of Safety Aspects of High Temperature Thermal-Energy Storage Systems," PL-54-TE 76-1130, NSF, Ec. 1976

3. Bramlete, T., et al, "Survey of High Temperature Thermal Energy Storage," Sandia Laboratories, March 1976

4. Eichelberger, J. L., "Investigation of Metal Fluoride Thermal Energy Storage Materials," Progress Report, ERDA Oct. 1976

5. Maru, H. C., et al "Molten Salt Thermal Energy Storage Systems: Salt Selection," ERDA, August 1976

6. Stepler, R., "Revolving Barrel Banks Solar Heat," Popular Science, May 1973

    Littlewood, R., and Edeleanu, C., "Thermodynamics of Corrosion in Fused Chlorides," Electrochemical Acta, Vol. 3, 1960

8. Susskind, H., et al, "Combating Corrosion in Molten Extraction Processes," Chemical Engineering Progress, Vol. 56, No. 3, March 1960

9. Borucka, A., Consulting Report to Grumman Aerospace Corp., February 10, 1977

10. Borucka, A., "Survey and Selection of Inorganic Salts for Application to Thermal Energy Storage," ERDA, June 1975

11. Kirst, W. E., et al, "A New Heat Transfer Medium for High Temperatures," ACS Meeting, May 1940

12. Technical Bulletin J-9, Park Chemical Company, Detroit, MI, 1976

13. Salt Price Sheets, Croton Chemical Company, South Plainfield, NJ, January 1977

14. Littlewood, R., J. Electrochem. Soc., Vol. 109, No. 6, June 1962